

- of the short arm of chromosome 4, *Exp. Hematol.* 31 (2003) 211–217.
- [10] T.M. Buttke, P.A. Sandstrom, Oxidative stress as a mediator of apoptosis, *Immunol. Today* 15 (1994) 7–10.
- [11] M. Patel, B.J. Day, J.D. Crapo, I. Fridovich, J.O. McNamara, Requirement for superoxide in excitotoxic cell death, *Neuron* 16 (1996) 345–355.
- [12] G. Fiskum, Mitochondrial participation in ischemic and traumatic neural cell death, *J. Neurotraum.* 17 (2000) 843–855.
- [13] J. Yuan, B.A. Yankner, Apoptosis in the nervous system, *Nature* 407 (2000) 802–809.
- [14] G. Rothe, G. Valet, Flow cytometric analysis of respiratory burst activity in phagocytes with hydroethidine and 2',7'-dichlorofluorescein, *J. Leukoc. Biol.* 47 (1990) 440–448.
- [15] N. Zamzami, P. Marchetti, M. Castedo, D. Decaudin, A. Macho, T. Hirsch, S.A. Susin, P.X. Petit, B. Mignotte, G. Kroemer, Sequential reduction of mitochondrial transmembrane potential and generation of reactive oxygen species in early programmed cell death, *J. Exp. Med.* 182 (1995) 367–377.
- [16] P.X. Petit, H. Lecoq, E. Zorn, C. Dauguet, B. Mignotte, M.L. Gougeon, Alterations in mitochondrial structure and function are early events of dexamethasone-induced thymocyte apoptosis, *J. Cell Biol.* 130 (1995) 157–167.
- [17] M.A. Barry, J.E. Reynolds, A. Eastman, Etoposide-induced apoptosis in human HL-60 cells is associated with intracellular acidification, *Cancer Res.* 53 (1993) 2349–2357.
- [18] J. Caceres-Cortes, D. Rajotte, J. Dumouchel, P. Haddad, T. Hoang, Product of the steel locus suppresses apoptosis in hemopoietic cells. Comparison with pathways activated by granulocyte macrophage colony-stimulating factor, *J. Biol. Chem.* 269 (1994) 12084–12091.
- [19] J. Li, A. Eastman, Apoptosis in an interleukin-2-dependent cytotoxic T lymphocyte cell line is associated with intracellular acidification. Role of the Na(+)/H(+)-antiport, *J. Biol. Chem.* 270 (1995) 3203–3211.
- [20] D. Perez-Sala, D. Collado-Escobar, F. Mollinedo, Intracellular alkalinization suppresses lovastatin-induced apoptosis in HL-60 cells through the inactivation of a pH-dependent endonuclease, *J. Biol. Chem.* 270 (1995) 6235–6242.
- [21] R.A. Gottlieb, H.A. Giesing, J.Y. Zhu, R.L. Engler, B.M. Babior, Cell acidification in apoptosis: granulocyte colony-stimulating factor delays programmed cell death in neutrophils by up-regulating the vacuolar H(+)-ATPase, *Proc. Natl. Acad. Sci. U.S.A.* 92 (1995) 5965–5968.
- [22] D.W. van Bekkum, Radiation sensitivity of the hemopoietic stem cell, *Radiat. Res.* 128 (1991) 4–8.
- [23] L.W. Terstappen, S. Huang, M. Safford, P.M. Lansdorp, M.R. Loken, Sequential generations of hematopoietic colonies derived from single nonlineage-committed CD34+CD38– progenitor cells, *Blood* 77 (1991) 1218–1227.
- [24] A.A. Cardoso, M.L. Li, P. Batard, A. Hatzfeld, E.L. Brown, J.P. Levesque, H. Sookdeo, B. Panterne, P. Sansilvestri, S.C. Clark, et al., Release from quiescence of CD34+ CD38– human umbilical cord blood cells reveals their potentiality to engraft adults, *Proc. Natl. Acad. Sci. U.S.A.* 90 (1993) 8707–8711.
- [25] Z. Darzynkiewicz, S. Bruno, G. Del Bino, W. Gorczyca, M.A. Hotz, P. Lassota, F. Traganos, Features of apoptotic cells measured by flow cytometry, *Cytometry* 13 (1992) 795–808.
- [26] W. Gorczyca, J. Gong, Z. Darzynkiewicz, Detection of DNA strand breaks in individual apoptotic cells by the in situ terminal deoxynucleotidyl transferase and nick translation assays, *Cancer Res.* 53 (1993) 1945–1951.
- [27] F.J. Herndon, H.C. Hsu, J.D. Mountz, Increased apoptosis of CD45RO- T cells with aging, *Mech. Age. Dev.* (1997) 94.
- [28] S. Miltenyi, W. Muller, W. Weichel, A. Radbruch, High gradient magnetic cell separation with MACS, *Cytometry* 11 (1990) 231–238.
- [29] E.A. Musgrove, D.W. Hedley, Measurement of intracellular pH, *Methods Cell Biol.* 33 (1990) 59–69.
- [30] K. Nagafuji, T. Shibuya, M. Harada, S. Mizuno, K. Takenaka, T. Miyamoto, T. Okamura, H. Gondo, Y. Niho, Functional expression of Fas antigen (CD95) on hematopoietic progenitor cells, *Blood* 86 (1995) 883–889.
- [31] D. Josefsen, J.H. Myklebust, D.H. Lynch, T. Stokke, H.K. Blomhoff, E.B. Smeland, Fas ligand promotes cell survival of immature human bone marrow CD34+CD38– hematopoietic progenitor cells by suppressing apoptosis, *Exp. Hematol.* 27 (1999) 1451–1459.
- [32] V. Settee, S. Hussein, L. Broody-Robinson, K. Allampallam, S. Mundle, R. Borok, E. Broderick, L. Mazzoran, F. Zorat, A. Raza, Intramedullary apoptosis of hematopoietic cells in myelodysplastic syndrome patients can be massive: apoptotic cells recovered from high-density fraction of bone marrow aspirates, *Blood* 96 (2000) 1388–1392.
- [33] J.W. Lee, G.M. Gersuk, P.A. Kiener, C. Beckham, J.A. Ledbetter, H.J. Deeg, HLA-DR-triggered inhibition of hemopoiesis involves Fas/Fas ligand interactions and is prevented by c-kit ligand, *J. Immunol.* 159 (1997) 3211–3219.
- [34] J. Domen, I.L. Weissman, Hematopoietic stem cells need two signals to prevent apoptosis; BCL-2 can provide one of these, Kitl/c-Kit signaling the other, *J. Exp. Med.* 192 (2000) 1707–1718.
- [35] S. Matsuyama, J. Llopis, Q.L. Deveraux, R.Y. Tsien, J.C. Reed, Changes in intramitochondrial and cytosolic pH: early events that modulate caspase activation during apoptosis, *Nat. Cell Biol.* 2 (2000) 318–325.
- [36] L.A. Smets, J. Van den Berg, D. Acton, B. Top, H. Van Rooij, M. Verwijs-Janssen, BCL-2 expression and mitochondrial activity in leukemic cells with different sensitivity to glucocorticoid-induced apoptosis, *Blood* 84 (1994) 1613–1619.
- [37] C. Richter, M. Schweizer, A. Cossarizza, C. Franceschi, Control of apoptosis by the cellular ATP level, *FEBS Lett.* 378 (1996) 107–110.
- [38] M. Leist, B. Single, A.F. Castoldi, S. Kuhnle, P. Nicotera, Intracellular adenosine triphosphate (ATP) concentration: a switch in the decision between apoptosis and necrosis, *J. Exp. Med.* 185 (1997) 1481–1486.
- [39] J.L. Lelli Jr., L.L. Becks, M.I. Dabrowska, D.B. Hinshaw, ATP converts necrosis to apoptosis in oxidant-injured endothelial cells, *Free Radic. Biol. Med.* 25 (1998) 694–702.
- [40] D.A. Bradbury, T.D. Simmons, K.J. Slater, S.P. Crouch, Measurement of the ADP:ATP ratio in human leukaemic cell lines

can be used as an indicator of cell viability, necrosis and apoptosis, *J. Immunol. Methods* 240 (2000) 79–92.

- [41] M. Comelli, F. Di Pancrazio, I. Mavelli, Apoptosis is induced by decline of mitochondrial ATP synthesis in erythroleukemia cells, *Free Radic. Biol. Med.* 34 (2003) 1190–1199.
- [42] M. Madesh, G. Hajnoczky, VDAC-dependent permeabilization of the outer mitochondrial membrane by superoxide induces rapid and massive cytochrome c release, *J. Cell Biol.* 155 (2001) 1003–1015.
- [43] B.M. Babior, NADPH oxidase: an update, *Blood* 93 (1999) 1464–1476.

# ***HLA* Genotyping Is Involved in Inter-individual Variations of NK Activity**

T. Hayashi\*, K. Imai\*, Y. Kusunoki\*, I. Hayashi\*\*,  
S. Kyoizumi\*, E. Tahara\* and K. Nakachi\*

*\*Department of Radiobiology/Molecular Epidemiology, Radiation Effects Research Foundation, Hiroshima, Japan, \*\*Central Research Laboratory, Hiroshima University Faculty of Dentistry, Hiroshima, Japan*

## **Summary**

We previously reported a higher incidence of cancer among individuals showing low NK activity of peripheral-blood lymphocytes than among those showing medium or high activity, based on a prospective cohort study among a Japanese general population (Lancet, 2000). In the present study, we focused on inter-individual variations in NK activity specifically looking at *HLA class I* (*HLA-A*, *HLA-B*, *HLA-C*). From 3,625 cohort members, we selected and compared two groups with high and low NK activity. Each group comprised 204 gender- and age-matched healthy individuals. We found statistically significant differences between the two groups in the frequency distribution of specific *HLA* genotypes: *B\*1301*, *B\*4403*, *B\*5401*, *Cw\*0401*, and *Cw\*07*. The results suggest that selected *HLA* genotypes are involved in determining individual NK activity.

## **Introduction**

The initial mechanism of immunosurveillance is thought to be a tumor-associated antigen non-specific cytotoxicity which includes natural killer (NK) cells. In numerous past laboratory studies on cancer immunosurveillance, there were clear indications of significant roles played by the natural cytotoxicity of various lymphocytes in preventing the development of cancer (1-5).

Based on a cohort study in a general population, we have shown that

NK activity is related to good health practices and that it plays an important role in immunological defense against cancer development (6, 7). We found large inter-individual differences in NK activity, 30% of which can be attributed to usual lifestyle, leaving the other factors unknown. A number of studies have determined that activation receptors of NK cells transmit activation signals through ligands on target cells, whereas inhibitory receptors recognize MHC class I (HLA class I in humans) and block activation signals. The self-recognition mechanisms of NK cells, however, remain unclear. The NK cell pool in one individual maintains an allotted number of NK cells that detect the expression of self-HLA class I, and the diverse repertoires of NK cells may be defined by different expressions of *KIR* and *CD94:NKG2D* genes that have specificity for self-HLA class I, this being in part determined by *HLA* genotyping of individuals (8). The involvement of HLA class I in NK cell repertoire selection leads to the hypothesis that HLA class I may play a role in determining individual NK cell activity. In this study, we examined this hypothesis in terms of NK activity and the frequency distribution of *HLA class I* (*HLA-A*, *HLA-B*, and *HLA-C*) genotypes, observed in a cohort study.

## Subjects and Methods

The Saitama cohort study consisted of 3,625 Japanese individuals living in a town in Saitama Prefecture; the NK activity of their peripheral-blood mononuclear cells was measured. This study is described in detail elsewhere (6, 7). The subjects gave peripheral-blood samples between 1986 and 1990, and these samples were immediately subjected to various immunological and biochemical assays, including NK activity, which was categorized into high, medium, and low levels by tertiles. A genome approach was recently undertaken in the Saitama cohort study, and we compared the high and low NK activity of two groups whose DNA of peripheral lymphocytes were available. Each group consisted of 204 cohort members without cancer history, who were age- and gender-matched to cancer cases.

This study was approved by the Genome Ethical Committee at Radiation Effects Research Foundation.

The assay method of NK activity is described elsewhere (7). In brief, effector cells were mononuclear lymphocytes, isolated from peripheral-blood samples of individual participants; target cells were K562, which were labeled with chromium 51. Percent specific lysis was calculated according to the standard formula, based on the amount of isotope released from lysed target cells.

Genomic DNA was extracted from peripheral-blood samples, and the *HLA* Typing kit (Wakunaga Pharmaceutical Co. Ltd., Hiroshima Japan) was used to determine each *HLA class I* genotype.

## Results and Discussion

We compared these two control groups in terms of *HLA class I* genotype frequencies. Tables show each *HLA* genotyping in the two groups with high and low NK activity. The distribution of each *HLA class I* genotype in the entire subject population was similar to the distribution among the general Japanese population reported so far. Among *HLA-A* genotypes, we did not find any statistically significant association with NK activity. (Table 1). Among *HLA-B* genotypes, *B\*1301*, *B\*4403*, and *B\*5401* zygosity showed a statistically significant association with NK activity ( $p = 0.02$ ,  $0.02$ , and  $0.04$ , respectively, Table 2). *B\*4403*, in particular, is relatively frequent among Japanese, and it has previously been suggested as being involved in the maturation of NK cells and thus the NK cell number. Among *HLA-C* genotypes, *Cw\*04* and *Cw\*07* revealed a significant association with NK activity ( $p = 0.03$  and  $0.01$ , respectively, Table 3). *Cw07* had previously been reported to be associated with a smaller subset of NK cells ( $CD16^+CD56^+$ ) (9). No other significant associations were found, but the results suggest that *HLA class I* genotypes may be associated with inter-individual differences in immunological competence and may therefore play a role in individual differences in innate immunity.

One general finding was that NK cells cannot kill cells expressing a full complement of autologous MHC class I allotypes, but can kill cells expressing some combination of allogenic MHC class I (10). It has

**Table 1** *HLA-A* genotyping in groups with high and low NK activity

<i>HLA-A</i> Genotypes	Low NK* n (%)	High NK* n (%)	P	Japanese** %
A*0101	1 (0.2)	0 (0.0)	0.50	0.6
A*02	99 (24.3)	93 (22.8)	0.62	23.7
A*0301	1 (0.2)	3 (0.7)	0.31	0.6
A*1101	30 (7.4)	31 (7.6)	0.89	9.3
A*2402	162 (39.7)	142 (34.8)	0.15	37.8
A*2601	47 (11.5)	50 (12.3)	0.75	10.9
A*3101	34 (7.3)	43 (10.5)	0.28	8.9
A*3303	34 (8.3)	46 (11.3)	0.16	7.5

\*Total n = 408 chromosomes (204 individuals). Low NK activity (in percent specific lysis): men (mean 29.6, range 5 - 42), women (mean 23.8, range 8 - 34). High NK activity: men (mean 68.5, range 59 - 90), women (mean 60.1, range 52 - 85)

\*\* From the report of the 11<sup>th</sup> Japan HLA Workshop (n=523).

**Table 2 HLA-B genotyping in control groups with high and low NK activity**

HLA-B Genotypes	Low NK* n (%)	High NK* n (%)	P	Japanese** %
B*0702	15 (3.7)	21 (5.1)	0.31	5.6
B*1301	0 (0.0)	6 (1.5)	<b>0.02</b>	1.5
B*15	51 (12.5)	36 (8.8)	0.09	8.9
B*2704	0 (0.0)	1 (0.2)	0.50	0.4
B*3501	39 (9.6)	25 (6.1)	0.07	7.2
B*3701	3 (0.7)	0 (0.0)	0.08	0.7
B*3802	1 (0.2)	0 (0.0)	0.50	n.a.
B*39	20 (4.9)	22 (5.4)	0.75	4.2
B*40	80 (19.6)	71 (17.4)	0.42	18.5
B*4403	28 (6.9)	48 (11.8)	<b>0.02</b>	7.4
B*4601	18 (4.4)	27 (6.6)	0.17	4.2
B*4801	9 (2.2)	8 (2.0)	0.81	2.4
B*5101	33 (8.1)	40 (9.8)	0.39	9.8
B*5201	60 (14.7)	54 (13.2)	0.55	11.3
B*5401	27 (6.6)	14 (3.4)	0.04	8.3
B*5502	5 (1.2)	9 (2.2)	0.28	2.6
B*56	5 (1.0)	3 (0.7)	0.36	0.9
B*5801	5 (1.2)	7 (1.7)	0.56	0.6
B*5901	7 (1.7)	9 (2.2)	0.61	1.9
B*6701	2 (0.5)	7 (1.7)	0.09	1.2

\* Total n = 408 chromosomes (204 individuals)

\*\* From the report of the 11<sup>th</sup> Japan HLA Workshop (n=523).

**Table 3 HLA-C genotyping in control groups with high and low NK activity**

HLA-C Genotypes	Low NK* n (%)	High NK* n (%)	P	Japanese** %
Cw*01	67 (16.4)	66 (16.2)	0.92	16.6
Cw*0202	0 (0.0)	1 (0.2)	0.50	n.a.
Cw*03	106 (26.0)	87 (21.3)	0.12	27.0
Cw*0401	19 (4.7)	8 (2.0)	<b>0.03</b>	4.4
Cw*0501	1 (0.2)	5 (1.2)	0.10	0.4
Cw*0602	2 (0.5)	0 (0.0)	0.25	1.3
Cw*07	40 (9.8)	64 (15.7)	<b>0.01</b>	11.7
Cw*08	45 (11.0)	33 (8.1)	0.15	11.1
Cw*1202	60 (14.7)	56 (13.7)	0.69	11.1
Cw*1402	30 (7.4)	31 (7.6)	0.89	4.8
Cw*1403	28 (6.9)	41 (10.0)	0.10	7.1
Cw*15	9 (2.9)	16 (3.9)	0.16	4.4

\* Total n = 408 chromosomes (204 individuals)

\*\* From the report of the 11<sup>th</sup> Japan HLA Workshop (n=523).

been reported that NK cell repertoires are defined by combinations of variable *KIR* and *HLA class I* genes and conserved *CD94:NKG2D* genes, and that the proportion of NK cells expressing various Ly49 molecules is also affected by the class I environment (8). Our results indicate that selected *HLA class I* genotypes are involved in determining the NK activity of individuals, which may correlate to NK cell numbers: This would imply that these genotypes are also associated with immunogenetical susceptibility to disease development, especially cancer. In addition, we also found in the cohort study that *NKG2D* haplotypes were closely associated with NK activity. In future, the combination of *HLA* genotype and genetic polymorphisms of receptors on NK cells, such as *NKG2D*, will provide new insights into the understanding of individual differences in innate immunity.

## References

1. M. E. VAN DEN BROEK, D. KAGI, F. OSSENDORP et al.: Decreased tumor surveillance in perforin-deficient mice. *J Exp Med*, 184: 1781-1790, 1996.
2. M. J. SMYTH, K. Y. THIA, S. E. STREET et al.: Differential tumor surveillance by natural killer (NK) and NKT cells. *J Exp Med*, 191: 661-668, 2000.
3. A. S. DIGHE, E. RICHARDS, L. J. OLD et al.: Enhanced in vivo growth and resistance to rejection of tumor cells expressing dominant negative IFN gamma receptors. *Immunity*, 1: 447-456, 1994.
4. D. H. KAPLAN, V. SHANKARAN, A. S. DIGHE et al.: Demonstration of an interferon gamma-dependent tumor surveillance system in immunocompetent mice. *Proc Natl Acad Sci U S A*, 95: 7556-7561, 1998.
5. V. SHANKARAN, H. IKEDA, A. T. BRUCE et al.: IFN gamma and lymphocytes prevent primary tumour development and shape tumour immunogenicity. *Nature*, 410: 1107-1111, 2001.
6. K. NAKACHI and K. IMAI: Environmental and physiological influences on human natural killer cell activity in relation to good health practices. *Jpn J Cancer Res*, 83: 798-805, 1992.
7. K. IMAI, S. MATSUYAMA, S. MIYAKE et al.: Natural cytotoxic activity of peripheral-blood lymphocytes and cancer incidence: an 11-year follow-up study of a general population. *Lancet*, 356: 1795-1799, 2000.
8. H. G. SHILLING, N. YOUNG, L. A. GUETHLEIN et al.: Genetic control of human NK cell repertoire. *J Immunol*, 169: 239-247, 2002.
9. D. P. DUBEY, C. A. ALPER, N. M. MIRZA et al.: Polymorphic Hh genes in the HLA-B(C) region control natural killer cell frequency and activity. *J Exp Med*, 179: 1193-1203, 1994.
10. N. M. VALIANTE, M. UHRBERG, H. G. SHILLING et al.: Functionally and structurally distinct NK cell receptor repertoires in the peripheral blood of two human donors. *Immunity*, 7: 739-751, 1997.

# Anisomycin downregulates gap-junctional intercellular communication via the p38 MAP-kinase pathway

Takahiko Ogawa<sup>1,\*</sup>, Tomonori Hayashi<sup>1</sup>, Seishi Kyoizumi<sup>1</sup>, Yoichiro Kusunoki<sup>1</sup>, Kei Nakachi<sup>1</sup>, Donald G. MacPhee<sup>1</sup>, James E. Trosko<sup>2</sup>, Katsuko Kataoka<sup>3</sup> and Noriaki Yorioka<sup>4</sup>

<sup>1</sup>Department of Radiobiology and Molecular Epidemiology, Radiation Effects Research Foundation, Hiroshima, Japan

<sup>2</sup>National Food Safety Toxicology Center, Department of Pediatrics/Human Development, Michigan State University, East Lansing, MI, USA

<sup>3</sup>Department of Histology and Cell Biology, Graduate School of Biomedical Sciences, Hiroshima University, Hiroshima, Japan

<sup>4</sup>Department of Molecular and Internal Medicine, Graduate School of Biomedical Sciences, Hiroshima University, Hiroshima, Japan

\*Author for correspondence (e-mail: tk-ogawa@hph.pref.hiroshima.jp)

Accepted 11 December 2003

Journal of Cell Science 117, 2087-2096 Published by The Company of Biologists 2004

doi:10.1242/jcs.01056

## Summary

Phosphorylation of connexin 43 (Cx43) molecules (e.g. by extracellular signal-regulated kinase) leads to reductions in gap-junctional intercellular communication (GJIC). GJIC levels also appear to be lower in the presence of p38 mitogen-activated protein (MAP) kinase, for unknown reasons. In this study, we used assays of the recovery of fluorescence by photobleached WB-F344 cells to demonstrate that GJIC levels are decreased by anisomycin [a protein synthesis inhibitor as well as an activator of p38 MAP kinase and c-Jun N-terminal kinases (JNK)] as a result of time-dependent depletion of the phosphorylated forms of Cx43. Using immunohistochemistry, we also detected far less of the Cx43 proteins at cell borders. These findings agree with the photobleaching assay results. Moreover, prior treatment with SB203580 (a specific inhibitor of p38 MAP kinase) appeared to be effective in preventing the loss of phosphorylated forms of Cx43 and the loss of Cx43 proteins at cell borders. Total protein labelling with [<sup>35</sup>S]-methionine and [<sup>32</sup>P]-orthophosphates

labelling of Cx43 showed that anisomycin enhanced the phosphorylation level of Cx43 along with inhibition of protein synthesis. SB203580 prevented the former but not the latter. The effect of anisomycin on GJIC was not dependent on the inhibition of protein synthesis because the addition of SB203580 completely maintained the level of GJIC without restoring protein synthesis. The Cx43 phosphorylation level increased by anisomycin treatment, whereas the amount of phosphorylated forms of Cx43 decreased, suggesting that activation of Cx43 phosphorylation might lead to the loss of Cx43. These results suggest that activation of p38 MAP kinase leads to reduction in the levels of phosphorylated forms of Cx43, possibly owing to accelerated degradation, and that these losses might be responsible for the reduction in numbers of gap junctions and in GJIC.

Key words: p38 MAP kinase, Connexin 43, GJIC, Anisomycin, SB203580, Protein synthesis inhibition

## Introduction

Gap junctions consist of plasma-membrane-spanning channels that permit the intercellular exchange of ions and low molecular weight molecules (Loewenstein, 1990). Gap-junctional intercellular communication (GJIC) is therefore believed to be involved in cell growth and differentiation; aberrant control might also play an important role in cancer development (Loewenstein, 1990; Trosko and Ruch, 1998). The mechanisms that regulate GJIC are not yet fully understood, although there is evidence that post-translational alterations of the connexins are involved (Musil and Goodenough, 1991; Musil and Goodenough, 1993; Trosko and Ruch, 1998). Connexin 43 (Cx43) is a widely expressed gap-junction protein found in many animal organs (Beyer et al., 1987; Dupont et al., 1991) and many recent investigations into the relationships between Cx43 phosphorylation and events in gap-junction assembly (channel gating) suggest that several protein kinases are capable of mediating both Cx43 phosphorylation and GJIC inhibition (Berthoud et al., 1993;

Cho et al., 2002; Hossain et al., 1998a; Kanemitsu and Lau, 1993; Laird et al., 1995; Lau et al., 1992; Musil et al., 1990; Musil and Goodenough, 1991; Musil and Goodenough, 1993; Trosko and Ruch, 1998; Warn-Cramer et al., 1998; Warn-Cramer et al., 1996).

The mitogen-activated protein (MAP) kinase belongs to an important family of protein kinases that act by phosphorylating specific amino acids on their target substrates. Of the classic MAP kinases, extracellular signal-regulated protein kinases 1 and 2 (ERK) are especially well known and can be activated by various physiological stimuli, including some growth factors (Seeger and Krebs, 1995). Previous investigations have shown that activation of ERK is an important element in the regulation of both GJIC and Cx43 (Berthoud et al., 1993; Hossain et al., 1998b; Hossain et al., 1999a; Kanemitsu and Lau, 1993; Lau et al., 1992; Ruch et al., 2001; Warn-Cramer et al., 1996; Warn-Cramer et al., 1998) but other studies investigating a range of ERK activators and inhibitors suggest that the correlation between ERK activation, Cx43 phosphorylation and GJIC



inhibition is by no means perfect (Hii et al., 1995a; Hii et al., 1995b; Hossain et al., 1998a; Hossain et al., 1999a). Previous evidence (Hii et al., 1995b; Matesic et al., 1994) indicates that Cx43 hyperphosphorylation by ERK activation, as indicated by a reduction in the mobility [on sodium dodecyl sulfate (SDS) gels] of the resulting Cx43 derivatives, is one mechanism of GJIC disruption available to cells, but it seems likely that other mechanisms of disruption, not necessarily dependent on Cx43 hyperphosphorylation, can and do exist.

We believe that other kinases and/or cofactors might be involved in the process of GJIC disruption; it is even possible that GJIC blockage is dependent upon the coordinated action of different MAP kinases, including ERK. Other members of the MAP-kinase family might also be involved (Cano and Mahadevan, 1995). Of these, p38 MAP kinase is the most obvious candidate, if only because of its involvement in signal transduction pathways that work in parallel with ERK (with which it shares ~50% sequence identity) (Tong et al., 1997). Given that these two signal transduction pathways overlap and 'cross talk' (Cano and Mahadevan, 1995; Helliwell et al., 2000; Töröcsik and Szeberényi, 2000), it seems reasonable to postulate a role for both p38 MAP kinase and ERK in the downregulation of Cx43 and/or the disruption of GJIC. Two recent reports, one suggesting that p38 MAP kinase is involved in GJIC upregulation and a second suggesting its involvement in GJIC downregulation (Cho et al., 2002; Polontchouk et al., 2002), are difficult to interpret because different cell types were used. Such contradictory findings do little if anything to clarify the relationship between p38 MAP kinase and GJIC regulation, and we thus designed a new study that we hoped would allow us to determine whether p38 MAP kinase contributes to Cx43 phosphorylation and/or gap-junctional disruption and, if so, how.

As a first step, we decided to examine the effects of anisomycin on GJIC. This interesting compound is well known to act as a protein synthesis inhibitor and a pharmacologically specific activator of two distinct kinds of kinases, p38 MAP kinase and c-Jun N-terminal kinases (JNKs) (Barros et al., 1997; Cano et al., 1994; Cano and Mahadevan, 1995; Hazzalin et al., 1998; Kyriakis et al., 1994), both of which can be stimulated by a wide variety of stress stimuli, including DNA damage, heat and osmotic shock, cytokines, and protein synthesis inhibitors (Minden and Karin, 1997). We also designed experiments in which we made use of a specific inhibitor of p38 MAP kinase, known as SB203580 (Cuenda et al., 1995; Tong et al., 1997), and other kinds of cell-to-cell-junction-related proteins, including ZO-1, occludin, E-cadherin and  $\beta$ -catenin. We also performed total cell metabolic labelling with [ $^{35}$ S]-methionine in order to try and rule out any possibility that the observed effects of anisomycin resulted from activation of the JNK pathway or a more general inhibitory effect on protein synthesis. Our findings strongly favour the hypothesis that p38 MAP kinase plays an important role in the disruption of GJIC by reducing the total amounts of phosphorylated Cx43, which effect is possibly due to accelerated degradation of phosphorylated Cx43 in the cells, and reducing the number of Cx43 proteins observed at cellular borders.

## Materials and Methods

### Cell culture

The Fisher 344 rat-liver-derived epithelial cell line WB-F344 (Tsao

et al., 1984) was cultured at 37°C in a 95% O<sub>2</sub>, 5% CO<sub>2</sub> atmosphere in a modified Eagle's medium (MEM) supplemented with 7% foetal calf serum (FCS), 50 U ml<sup>-1</sup> penicillin and 50 µg ml<sup>-1</sup> streptomycin sulfate. Passage 8-21 cells were used in all experiments.

### Materials

Anisomycin (2-*p*-methoxyphenylmethyl-3-acetoxy-4-hydroxy-pyrrolidine) and dimethyl sulfoxide (the vehicle for SB203580) were from Sigma (St Louis, MO) and SB203580 [4-(4-fluorophenyl)-2-(4-methylsulphonylphenyl)-5-(4-pyridyl) imidazole] was from Calbiochem (La Jolla, CA). PhosphoPlus p38 MAP kinase and SAPK/JNK Antibody Kit™ were from Cell Signaling Technology (Beverly, MA). Carboxyfluorescein diacetate (CFDA) was from Molecular Probes (Eugene, OR). Lab-Tek Chamber Slides™ were from Nalge Nunc International (Naperville, IL). Anti-Cx43 monoclonal antibody and Alexa-488-conjugated goat anti-mouse antibody were from Chemicon International (Temecula, CA) and Molecular Probes (Eugene, OR), respectively. Anti-ZO-1 and anti-occludin polyclonal antibodies (Zymed Laboratories, San Francisco, CA), and anti-E-cadherin (Transduction Laboratories, Lexington, KY), anti- $\beta$ -catenin (Zymed Laboratories), anti- $\beta$ -actin (Sigma) monoclonal antibodies were also used. SDS polyacrylamide-gel electrophoresis (SDS-PAGE) supplies and reagents for western blot analyses were from Bio-Rad (Richmond, CA). The enhanced chemiluminescence detection kit was from Renaissance Western Blot Chemiluminescence Reagent (NEN Life Science Products, Boston, MA). [ $^{35}$ S]-Methionine and [ $^{32}$ P]-orthophosphates were from Perkin Elmer Life and Analytical Sciences (Boston, MA).

### Cell treatments with anisomycin and SB203580

WB-F344 cells seeded in dishes or slides were grown to approximately 80% confluence. The medium was replaced with fresh medium containing 0.2% FCS and the cells were then incubated for a further 48 hours. Cells were treated with 10 µg ml<sup>-1</sup> (10 mg ml<sup>-1</sup> stock in distilled water) anisomycin for 5, 30, 60, 90, 120 and 180 minutes at 37°C. To block the p38 MAP kinase, cells were treated with 10 µM SB203580 (50 mM stock in dimethyl sulfoxide) for 30 minutes at 37°C before being exposed to anisomycin for 60 minutes. Controls for the experiments were treated with 0.02% dimethyl sulfoxide and/or distilled water. Aliquots of the treated cell suspensions were then used for measurements of GJIC, MAP kinase activation levels, Cx43 phosphorylation levels and immunofluorescence.

### FRAP assay for GJIC

Our procedure was a modified version of the standard method for measuring GJIC by quantitative fluorescence recovery after photobleaching (FRAP) (Ogawa et al., 1999; Trosko et al., 2000; Wade et al., 1986). Assays were performed using an ACAS Ultima laser cytometer (Meridian Instruments, Okemos, MI). After selectively bleaching cells with a micro-laser beam, we followed the rate of transfer of CFDA from adjacent labelled cells back into bleached cells. Recovery of fluorescence was assessed at 1-minute intervals and recovery rates (RRs) were calculated as percentages of fluorescence recovered per minute. Anisomycin and/or SB203580 were not present in the medium during labelling of the cells with CFDA, photobleaching or calculation of RR. All calculated rates were corrected for the loss of fluorescence by unbleached control cells and the results expressed as the average percentage (mean±s.e.m.) recovery rate of treated cells relative to the recovery rate of untreated cells.

### Indirect immunofluorescence and confocal microscopy

WB-F344 cells were cultured as previously described (Trosko et al.,

2000) and the cells plated on a Lab-Tek Chamber Slide™ for anisomycin and/or SB203580 treatment. After treatment, the cells were washed twice in PBS and fixed in periodate-lysine-paraformaldehyde fixative for 30 minutes; they were then washed and permeabilized three times with 0.1% Triton-X-100/PBS (PBST), and incubated in 20% BlokAce (Dainihon Pharmaceuticals, Tokyo, Japan) for 1 hour. The next stage involved overnight incubation at 4°C in a 1:2000 dilution of anti-Cx43 monoclonal antibody (Chemicon) followed by three washes with PBST before incubation in Alexa-488-conjugated goat anti-mouse antibody (Molecular Probes) at a dilution of 1:2000 for 1 hour in dark conditions. The cells were then washed three times in PBST and once in PBS before being mounted in Gel/Mount (Biomed, Foster City, CA) for examination in a Zeiss LSM 510 laser-scanning confocal microscope.

#### Immunoblotting

Cells grown to approximately 80% confluence in 10-cm dishes were treated with anisomycin, anisomycin plus SB203580, or SB203580 plus either distilled water or dimethyl sulfoxide as the vehicle control. At the end of the treatment period, the monolayers were rinsed three times with ice-cold PBS. Lysates were prepared with ice-cold lysis buffer containing 20 mM Tris-buffered saline (TBS), pH 7.5, 1% Triton X-100, 150 mM NaCl, 1 mM each of EDTA, EGTA,  $\beta$ -glycerophosphate,  $\text{Na}_3\text{VO}_4$  and phenylmethyl-sulfonyl fluoride (PMSF), 2.5 mM sodium pyrophosphate, and 1  $\mu\text{M}$  leupeptin, and then sonicated. The samples were diluted 1:5 in water and their protein concentrations determined using the DC protein assay™ (Bio-Rad). Samples (20  $\mu\text{g}$ ) of protein were then dissolved in Laemmli sample buffer, separated on 12.5% polyacrylamide gels, and transferred to polyvinylidene difluoride membranes (Bio-Rad) before determining their phosphorylated p38 MAP kinase and JNK levels according to the manufacturer's protocols for PhosphoPlus p38 (Thr180/Tyr182) and SAPK/JNK (Thr183/Tyr185) MAP Kinase Antibody Kit™ (Cell Signaling Technology) assays. The Cx43 content of the various samples was also determined by incubating the samples with an anti-Cx43 monoclonal antibody (Chemicon; diluted 1:2000), and later adding a horseradish-peroxidase-conjugated secondary antibody (diluted 1:2000; Amersham, Arlington Heights, IL) and an enhanced chemiluminescence detection reagent (NEN Life Science Products). The membrane was stripped and reprobed with anti-ZO-1 and anti-occludin polyclonal antibodies (Zymed, diluted 1:2000), and anti-E-cadherin (Transduction, 1:2000), anti- $\beta$ -catenin (Zymed, 1:2000) and anti- $\beta$ -actin (Sigma, 1:2000) monoclonal antibodies, respectively. The average control value was assigned an arbitrary value of 1 unit and relative band intensities were standardized to this arbitrary unit (AU).

#### [<sup>35</sup>S]-Methionine total protein metabolic labelling of WB-F344 cultures

To confirm that anisomycin acts as a protein synthesis inhibitor *in vivo*, metabolic labelling of WB-F344 cells was conducted. Cells were starved of methionine for 30 minutes at 37°C in methionine-free MEM. The medium was then replaced with fresh labelling medium containing [<sup>35</sup>S]-methionine (0.1 mCi per 6 cm dish of cells) and incubation was continued for the final 60 minutes. Anisomycin and SB203580 were incubated for the last 60 or 90 minutes. The radioactive medium was removed after a pulse labelling and cells were rinsed with PBS and solubilized in cold RIPA buffer containing 2 mM sodium orthovanadate, 1 mM PMSF and 1% Triton-X-100. Cells were harvested and the DNA was sheared by drawing the lysate through a 26 G needle. After centrifugation, supernatant was collected and resuspended (1  $\mu\text{l}$ ) in 1 ml of scintillate followed by liquid scintillation spectrometry.

#### [<sup>32</sup>P]-Orthophosphate metabolic labelling of WB-F344 cultures

Radioimmunoprecipitation of Cx43 was performed as described

above. Cells were starved of phosphates for 30 minutes at 37°C in phosphate-free MEM and supplemented with 0.2% dialysed FCS. The medium was then replaced with fresh labelling medium containing [<sup>32</sup>P]-orthophosphate (0.1 mCi per 6 cm dish of cells) and preincubation was continued for 60 minutes. After the addition

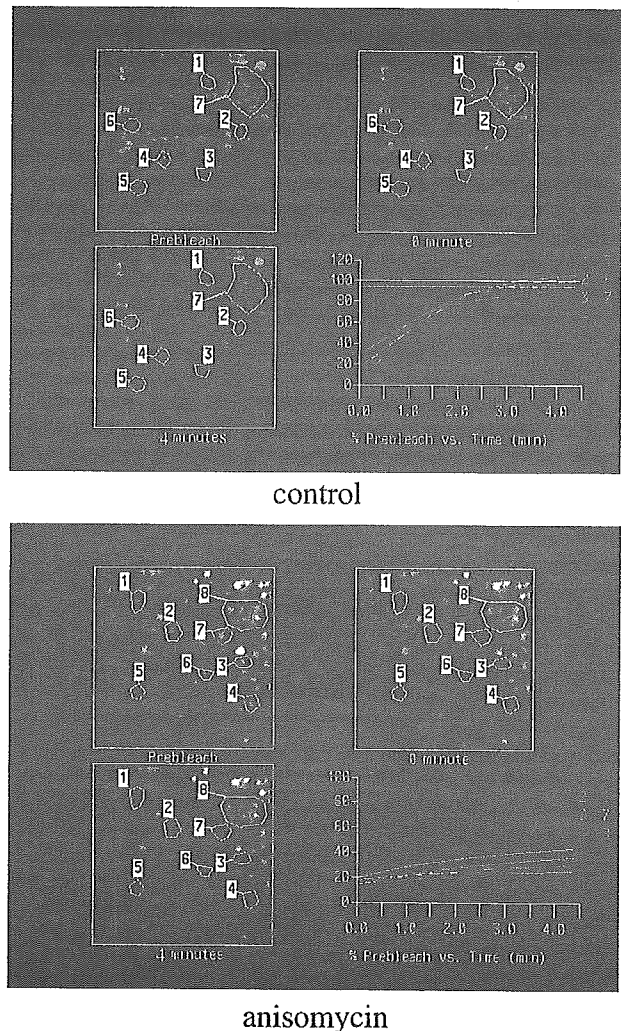


**Fig. 1.** Typical digitized fluorescence images and plots of fluorescence recovery after photobleaching. With (anisomycin) or without (control) anisomycin treatment for 60 minutes, cells were labelled with 5,6-carboxyfluorescein diacetate. Suitable fields of cells were identified using a 40 $\times$  objective lens. Such fields contained many cells that were in contact with each other but not too confluent. Each field was scanned to generate a digital image of fluorescence (Prebleach). After the initial scan, selected cells were photobleached (0 minute, numbers 1-6). Sequential scans were then carried out at 30 second intervals to detect recovery of fluorescence in the bleached cells (4 minute, numbers 1-6). Images were digitally recorded for analysis. Several unbleached cells were also monitored to provide control data (number 7). Typical plots of fluorescence recovery after photobleaching are shown (proportion of prebleaching against time). A rising slope indicates the recovery of fluorescence. The percentage recovery of fluorescence over time was determined for each selected cell and the data were corrected for the background loss of fluorescence in one area (number 7).

of anisomycin and/or SB203580, culture was continued in radioactive medium. Each treatment group was exposed to 0.02% dimethyl sulfoxide as vehicle alone for 90 minutes, anisomycin at  $10 \mu\text{g ml}^{-1}$  for 60 minutes, SB203580 plus anisomycin (pretreatment of SB203580 for 30 minutes, then co-treatment with anisomycin for an additional 60 minutes), or SB203580 alone for 90 minutes. Anisomycin and SB203580 were incubated for the last 60 or 90 minutes. The radioactive medium was removed after one pulse for three hours, and cells were rinsed with TBS and solubilized in cold RIPA buffer containing sodium orthovanadate (2 mM), 1 mM PMSF and 1% Triton-X-100. Cellular debris was concentrated by centrifugation (10 minutes, 20,400 g), and supernatant was collected and incubated with 20  $\mu\text{l}$  of a 50% slurry of Protein-G/Sepharose CL-4B (Amersham Pharmacia Biotech, Uppsala, Sweden) and the samples were rotated for 1 hour at room temperature. The samples were then centrifuged at 20,400 g for 10 minutes and the supernatant was collected and incubated with 1  $\mu\text{g}$  anti-Cx43 monoclonal antibody (Chemicon) for 1 hour, followed by addition of 20  $\mu\text{l}$  of the 50% slurry of Protein-G/Sepharose CL-4B for 1 hour. The immunoprecipitates were washed four times with TBS and supplemented with Laemli sample buffer and boiled at  $95^\circ\text{C}$  for 5 minutes. Samples, derived from equal volume of cell lysates, were electrophoresed on 12.5% SDS gels and autoradiographed. Phosphorylated bands were analysed by autoradiography using Personal Molecular Imager FX (Bio-Rad).

#### Densitometric analysis

Exposed films were scanned using a flatbed scanner and band density was analysed using NIH Image<sup>TM</sup>.

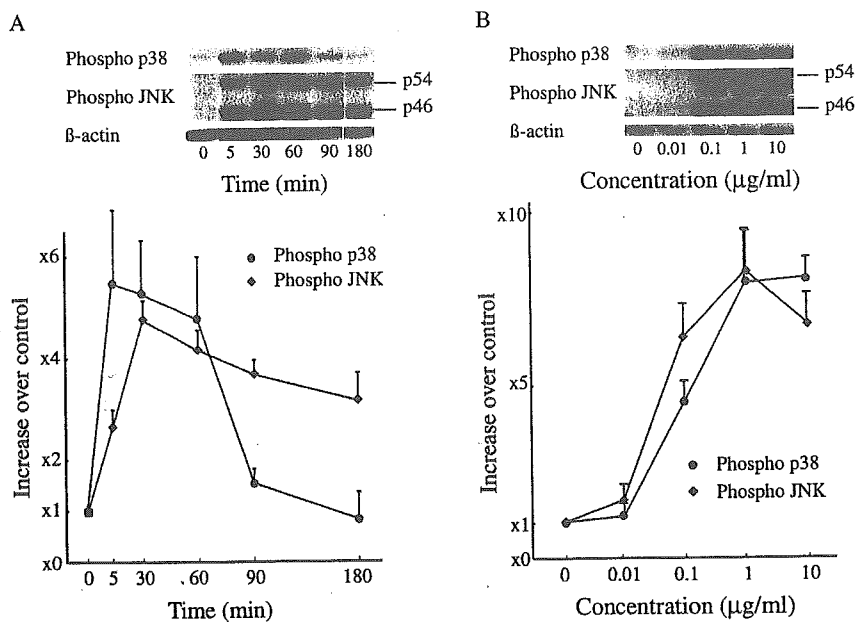


**Fig. 2.** Time (A) and dose (B) course analyses of the effect of anisomycin on MAP kinase activity. After treatment with anisomycin, cell lysates were prepared and 20  $\mu\text{g}$  protein was separated on 12.5% gel and transferred onto a PVDF membrane. The same membrane was probed and reprobbed after stripping with antibodies against doubly phosphorylated p38 MAP kinase, phosphorylated p46/p54 and  $\beta$ -actin as control in protein loading. These results were representative of three experiments, each performed with a different preparation of cells, and are expressed as the fold activity (means $\pm$ s.e.m.) of band density relative to that of untreated control by densitometric analysis.

#### Statistical analysis

Data were analysed using Statview II software<sup>TM</sup> (Apple Computer, Cupertino, CA). The two-tailed unpaired Student's *t*-test was used in comparisons of the anisomycin- or SB203580-treated cultures with control cultures; differences were considered significant at  $P < 0.05$ . Results are expressed as the mean $\pm$ s.e.m.

#### Results

Typical digitized fluorescence images and plots of fluorescence recovery after photobleaching of untreated cells and cells treated with anisomycin for 60 minutes are shown in Fig. 1. The untreated cells recovered their fluorescence within 4 minutes, whereas the anisomycin treated cells did not.

To determine whether this anisomycin-induced effect is specifically related to the ability of anisomycin to activate p38 MAP kinase, we also examined the phosphorylation status of the other MAP kinase families. To do this, we assessed the activities of p38 MAP kinase and JNK by measuring the levels of their active phosphorylated forms using immunoblotting. Densitometric band analyses of the phosphorylated forms of p38 MAP kinase and JNK (p46/p54) are shown in Fig. 2. The time-course study shows that anisomycin treatment led to the phosphorylation of both p38 MAP kinase and JNK (Fig. 2A). Phosphorylation of p38 MAP kinase was not observed in the absence of anisomycin, a peak level being reached at 5 minutes and sustained until 60 minutes. Phosphorylated JNK levels increased much more slowly after anisomycin treatment, with a peak becoming evident at 30 minutes. The dose study shows that phosphorylated p38 MAP kinase and JNK increased at concentrations of more than  $0.1 \mu\text{g ml}^{-1}$ , with peaks of 8.1 times the control at  $10 \mu\text{g ml}^{-1}$  (p38 MAP kinase) and 8.3 times the control at  $1 \mu\text{g ml}^{-1}$  (JNK) (Fig. 2B).

We therefore used the FRAP assay to measure the RR at each time point as a simple way of quantifying the effects of anisomycin treatment on GJIC. The results were consistent: the addition of anisomycin ( $10 \mu\text{g ml}^{-1}$ ) to WB-F344 cells led to a time-dependent decrease in RR, in that there was a significant decrease to  $\sim 80\%$  of the control value at 5 minutes and then to  $\sim 55\%$  at 30 minutes and  $\sim 50\%$  at 60 minutes (this was the lowest level reached and was retained up to 180 minutes) (Fig. 3A). Cells that had been incubated for up to 60 minutes with the same concentration of anisomycin turned out to have near-normal RRs only 24 hours after the removal of the anisomycin (data not shown). To assess the dose effect of anisomycin, 60 minute assays were performed at various concentrations of anisomycin. There was no significant decrease at  $< 0.1 \mu\text{g ml}^{-1}$  but the RR decreased to about 75% of control at  $1 \mu\text{g ml}^{-1}$ , with

maximal effect at  $10 \mu\text{g ml}^{-1}$  (about 40% of control) (Fig. 3B). In order to assess effects of anisomycin concentrations on protein synthesis, we estimated the amount of proteins produced de novo using an [ $^{35}\text{S}$ ]-methionine metabolic labelling assay (Fig. 3C). There was a significant decrease in the total protein level even at the lowest concentration ( $10 \text{ ng ml}^{-1}$ ) of anisomycin by which p38 MAP kinase could not be activated (Fig. 2B). Thus, we could not dissociate the inhibition of protein synthesis from the GJIC downregulation by using

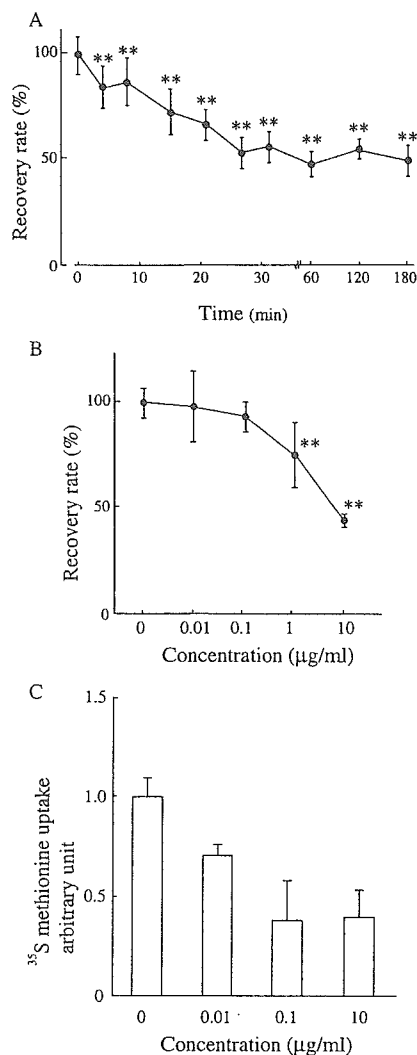


**Fig. 3.** Time (A) and dose (B) course analyses of the effect of anisomycin on GJIC. GJIC was estimated by FRAP in cells treated with anisomycin. Results are expressed as the percentage (mean $\pm$ s.e.m.) of RR relative to that of control cells (set to 100%) treated with distilled water. These results are representative of at least three experiments.  $**P < 0.01$  versus cells incubated with control. (C) To examine the effect of anisomycin as protein synthesis inhibitor, we used a [ $^{35}\text{S}$ ]-methionine metabolic labelling assay. At each concentration ( $0.01 \mu\text{g ml}^{-1}$ ,  $0.1 \mu\text{g ml}^{-1}$  and  $10 \mu\text{g ml}^{-1}$ ) of anisomycin, [ $^{35}\text{S}$ ]-labelled protein level was shown as radioactivity by liquid scintillation spectrometry. For comparison, the radioactivity of control was arbitrarily set at 1. Results were expressed as means $\pm$ s.e.m. of three separate experiments.

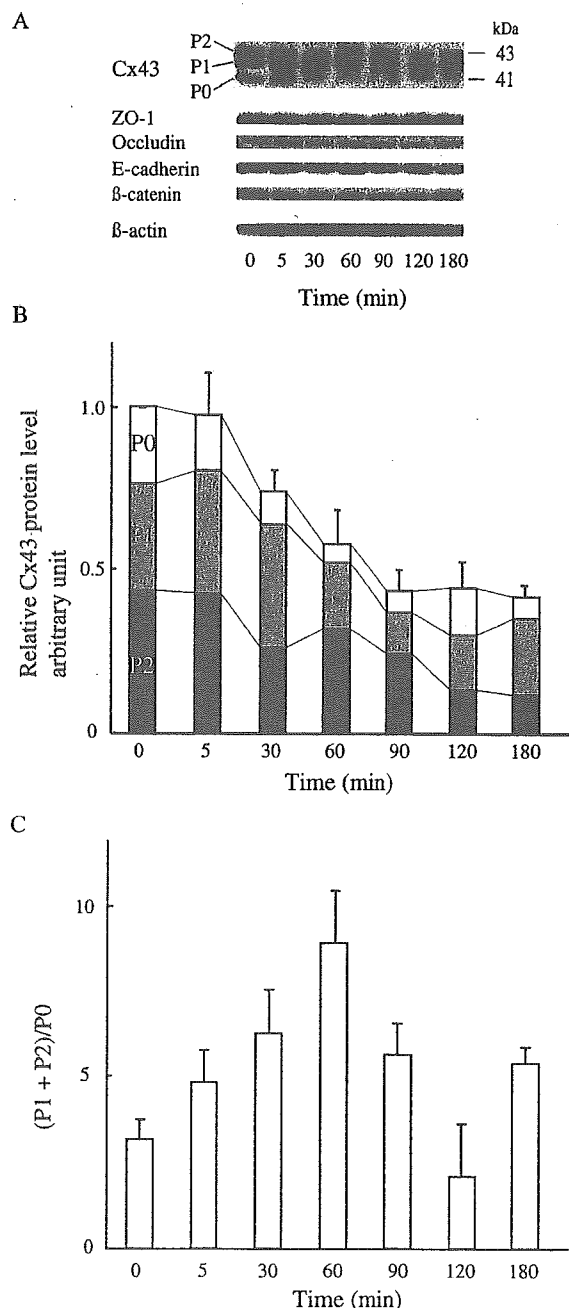


**Fig. 4.** Phosphorylation of Cx43 protein in anisomycin-treated cells. (A) Typical western blots of the Cx43 protein, with ZO-1, occludin, E-cadherin and  $\beta$ -catenin as reference proteins and  $\beta$ -actin as a control for protein loading. Numbers indicate the time from the addition of anisomycin. After incubation with anisomycin ( $10 \mu\text{g ml}^{-1}$ ) for 5, 30, 60, 90, 120 and 180 minutes, whole-cell extracts ( $20 \mu\text{g}$  per lane) were probed with antibodies. All samples show multiple Cx43 protein bands (P0, P1 and P2) depending on the phosphorylation level, and equal levels of reference proteins. (B) Densitometric analysis of the most important bands of Cx43 protein. The relative band intensities are shown. For assessment of each protein, the total amounts of control were arbitrarily set at 1. (C) Each column displays the ratio of (P1+P2):P0. Values are the means $\pm$ s.e.m. of three separate experiments.

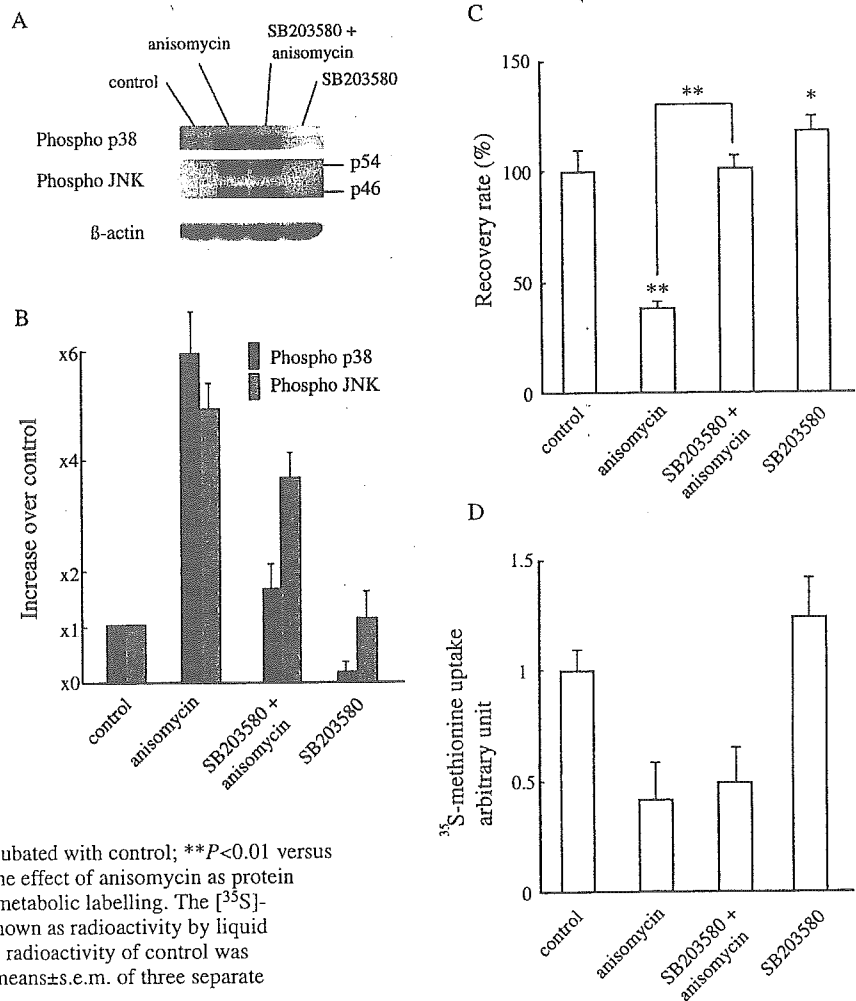
lower concentrations of anisomycin (around 25–50 ng ml<sup>-1</sup>; so-called subinhibitory level) that appeared to have an ability to activate the p38 MAP kinase.

An examination of the profiles of the various forms of Cx43 before and after anisomycin treatment led to some interesting findings. Before treatment, we could detect three predominant forms of the Cx43 protein by SDS-PAGE; each form could be seen as a distinct immunoreactive band of between 41 and 43 kDa. The minor unphosphorylated form of Cx43 (P0) migrated fastest, whereas the more abundant phosphorylated forms (P1 and P2) migrated more slowly (Fig. 4A), as noted previously (Trosko and Ruch, 1998). After setting the total Cx43 level of control cells at 1 AU, we noted that the combined intensities of P0, P1 and P2 had reached their lowest point (0.46 AU) at 90 minutes and retained up to 180 minutes. Following the addition of anisomycin, the absolute amount of the phosphorylated forms of Cx43 (i.e. P1+P2), and also of P0, tended to decrease time dependently until 120 minutes, which coincided almost precisely with the disruption of GJIC (Fig. 3A). By contrast, none of ZO-1, occludin, E-cadherin and  $\beta$ -catenin showed any changes. The ratios of P1+P2 to P0 were assayed at intervals throughout the course of a 180-minute treatment period. Although the ratio increased about ninefold,

reaching a peak at 60 minutes, it then decreased rapidly, only to increase again at 180 minutes (Fig. 4C). The disruption of GJIC that we were observing appeared to vary inversely with the absolute amounts of Cx43 phosphorylated forms P1+P2 and P0 that were present.

As expected, we were able to detect phosphorylation of p38 MAP kinase in anisomycin-treated cells not pretreated with SB203580, whereas cells treated with only SB203580 did not appear to contain any phosphorylated p38 MAP kinase whatsoever (Fig. 5A). The levels of p38 MAP kinase phosphorylation in normal cells were found to have increased about sixfold after anisomycin treatment, but only twofold or so in cells pretreated with SB203580 (Fig. 5B). Anisomycin treatment also led to significant increases (about fivefold) in JNK phosphorylation levels in normal cells. Although pretreatment with SB203580 led to somewhat smaller anisomycin-induced increases (about fourfold), there was every indication that SB203580 was far less effective at blocking JNK phosphorylation than it had been at blocking p38 MAP kinase phosphorylation. We found that cells pretreated with 10  $\mu$ M SB203580 for 30 minutes were no longer subject to the anisomycin-induced reductions in GJIC experienced by cells pretreated with SB203580-free medium (Fig. 5C). To

**Fig. 5.** SB203580 interferes with the effects of anisomycin p38 MAP kinase activity on GJIC. Each treatment group was exposed to 0.02% dimethyl sulfoxide as vehicle alone for 90 minutes (control), anisomycin at 10  $\mu$ g ml<sup>-1</sup> for 60 minutes, SB203580 plus anisomycin (pretreatment of SB203580 for 30 minutes, then co-treatment with anisomycin for an additional 60 minutes) or SB203580 alone for 90 minutes. Cells with or without pretreatment with SB203580 at 10  $\mu$ M were exposed to 10  $\mu$ g ml<sup>-1</sup> of anisomycin for 60 minutes. After treatment, samples were prepared as described in Fig. 2B. (A) Typical immunoblot analyses using specific antibodies against phosphorylated forms of p38 MAP kinase, JNK and  $\beta$ -actin as protein-loading control. (B) This result is representative of three experiments, each performed with a different preparation of cells and plotted as the fold activity (mean $\pm$ s.e.m.) of band density relative to that of control by densitometric analysis. (C) Results are expressed as the percentage (mean $\pm$ s.e.m.) of RR relative to that of control cells (100%) of at least three separate experiments. \* $P$ <0.05 versus cells incubated with control; \*\* $P$ <0.01 versus cells incubated with control. (D) To examine the effect of anisomycin as protein synthesis inhibitor, we used [<sup>35</sup>S]-methionine metabolic labelling. The [<sup>35</sup>S]-methionine-incorporated protein levels were shown as radioactivity by liquid scintillation spectrometry. For comparison, the radioactivity of control was arbitrarily set at 1. Results were expressed as means $\pm$ s.e.m. of three separate experiments.



determine whether SB203580 could inhibit the anisomycin-induced suppression of protein synthesis, we examined the [ $^{35}\text{S}$ ]-methionine contents of total cell lysates and found that SB203580 was not able to restore the level of protein synthesis to the control levels (Fig. 5D). Because the addition of

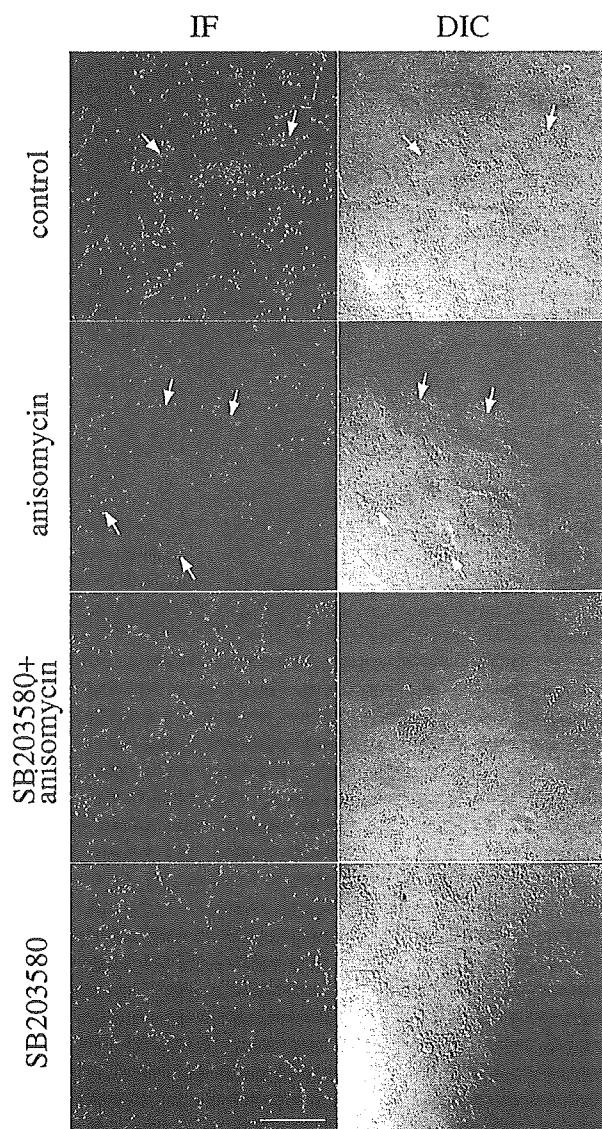


**Fig. 6.** Anisomycin introduced redistribution of Cx43 and gap-junction plaques. Cx43 was visualized as green spots by indirect immunofluorescence using FITC-labelled secondary antibody. Two sets of quadruple photographs are shown containing immunofluorescence images (IF) and Nomarski differential interference contrast images (DIC) of the same fields. These are typical images of each treatment group. Each treatment group was exposed to 0.02% dimethyl sulfoxide as vehicle alone for 90 minutes (control), anisomycin at  $10\ \mu\text{g ml}^{-1}$  for 60 minutes, SB203580 plus anisomycin (pretreatment of SB203580 for 30 minutes, then co-treatment with anisomycin for an additional 60 minutes) or SB203580 alone for 90 minutes. Cytoplasmic staining for Cx43 was also observed (indicated by white arrows). All images in each panel are of the same magnification. Scale bar,  $20\ \mu\text{m}$ .

SB203580 appeared to maintain the RR completely (Fig. 5C), it is most likely that the effect of anisomycin on GJIC was not dependent on the inhibition of protein synthesis.

The relationship between p38 MAP kinase phosphorylation/activation and the cellular distribution of Cx43 was assessed by indirect immunofluorescence with monoclonal antibodies in a confocal laser-scanning microscope. Cellular regions containing Cx43 protein molecules were readily identified as a series of brightly stained punctate maculae at the borders of unstimulated cells but significant quantities were located elsewhere (e.g. in a few small compartments adjacent to the nucleus – see the arrows in Fig. 6). By 60 minutes, there was much less Cx43 at most cell borders. These observations are consistent with the profile of anisomycin-induced GJIC loss as judged by FRAP assay results; moreover, the fact that Cx43 protein could still be detected close to cell nuclei after the addition of anisomycin seems to indicate that the anisomycin-induced decreases in GJIC were mostly a result of the loss of Cx43 molecules from cell borders, as opposed to losses from elsewhere in the cell. It is interesting that, as might have been predicted on the basis of our FRAP results, most of the losses of Cx43 molecules from the cell border regions detected in anisomycin-treated WB-F344 cells were not apparent in their SB203580-pretreated counterparts (Fig. 6).

Whole-cell lysates were prepared from cells exposed to SB203580 for 30 minutes before being incubated in the presence or absence of anisomycin. Equal amounts of protein ( $20\ \mu\text{g}$ ) were then extracted from each cell lysate and subjected to SDS-PAGE, immunoblotting and densitometric analyses (Fig. 7A,B). The cells that had been incubated with anisomycin for 60 minutes and, as a result, had lost half their capacity for GJIC turned out to have significantly reduced P1+P2 and P0 levels (Fig. 4). By contrast, cells exposed to  $10\ \mu\text{M}$  SB203580 before their anisomycin treatment seemed to lose very little of their P1 and P2. As expected, the P1 and P2 levels in cells exposed to SB203580 alone were virtually the same as those in the appropriate controls. Interestingly, pretreatment of cells with SB203580 did not seem to prevent anisomycin-induced loss of P0, despite their P1+P2 level appearing to be much the same in the presence and absence of anisomycin. We further analysed phosphorylation levels of Cx43 by [ $^{32}\text{P}$ ]-orthophosphate metabolic labelling (Fig. 7C). Incorporated [ $^{32}\text{P}$ ]-phosphates measured as relative radioactivity were augmented, despite the apparent decrease of phosphorylated forms of Cx43 at 60 minutes after anisomycin treatment. This implies that a Cx43 molecule incorporated more phosphates after anisomycin treatment than the untreated control. This phosphorylation augmentation could be almost completely inhibited by the addition of SB203580 (Fig. 7C), indicating that the excess phosphorylation caused by anisomycin is specific to activation of p38 MAP kinase.

## Discussion

To resolve the issue of whether p38 MAP kinase is involved in the post-translational regulation of GJIC, experiments were designed to examine whether anisomycin, an activator of p38 MAP kinase and an inhibitor to protein synthesis, could modulate GJIC in a diploid, non-tumorigenic rat liver epithelial cell line. We found that incubation with anisomycin led to marked reductions in GJIC in WB-F344 cells and that



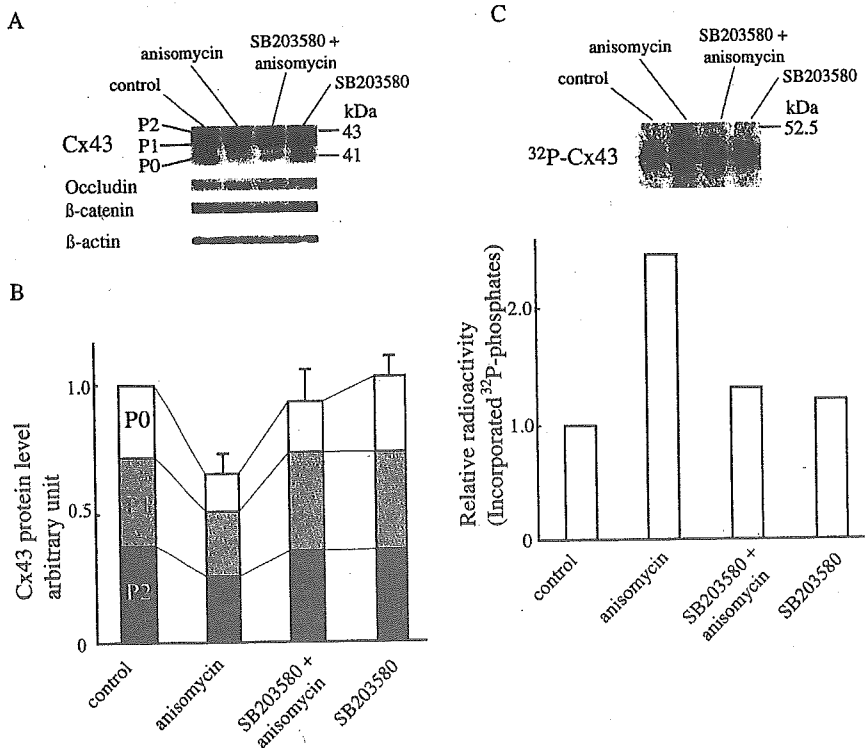


**Fig. 7.** Western blot analysis of Cx43 protein expression in cells treated with anisomycin and/or SB203580. Each treatment group was exposed to 0.02% dimethyl sulfoxide as vehicle alone for 90 minutes (control), anisomycin at 10  $\mu\text{g ml}^{-1}$  for 60 minutes, SB203580 plus anisomycin (pretreatment of SB203580 for 30 minutes, then co-treatment with anisomycin for an additional 60 minutes) or SB203580 alone for 90 minutes. (A) A typical western blot. Whole-cell extracts (20  $\mu\text{g}$  per lane) were probed with an antibody against Cx43 or against occludin,  $\beta$ -catenin as reference proteins, and against  $\beta$ -actin as a control for protein loading. (B) The relative band intensities of P1, P2 and P0 of Cx43. (C) Autoradiograph of [ $^{32}\text{P}$ ]-orthophosphate labelled Cx43 and its densitometric analysis on an SDS-PAGE gel. Results are from one representative experiment of two separate experiments. To assess each sample, the total value of control radiation was arbitrarily set at 1.

this reduction was accompanied by decreases of the phosphorylated Cx43 protein moieties with which WB-F344 cells are usually associated. The most obvious change involved significant reductions in the levels of the P1 and P2 forms of Cx43. These reductions were reflected in significant losses of Cx43 protein at cellular borders. Such findings are especially interesting in the light of suggestions by previous workers that activation of the ERK signalling pathway leads to hyperphosphorylation of Cx43 and that this in turn leads to reductions in GJIC (Hossain et al., 1998a; Hossain et al., 1999b; Kanemitsu and Lau, 1993; Warn-Cramer et al., 1998; Warn-Cramer et al., 1996).

We reported that GJIC levels are greatly reduced in human primary cultured cells by losses of phosphorylated Cx43 moieties (Ogawa et al., 2001). In the present study, we noted that the absolute levels of phosphorylated Cx43 molecules that we could detect were always significantly lower in anisomycin-treated cells whose GJIC levels had been reduced. This might mean that the decreases in GJIC that we observe in such circumstances are the result of decreases in intracellular levels of phosphorylated Cx43 moieties. Current understanding of gap junction assembly, stability and turnover is that the post-translational phosphorylation of Cx43, as shown by overall changes in species migration on SDS gels, is essential for the functioning of gap junction channels (Elvira et al., 1993; Hossain et al., 1998b; Musil et al., 1990). We therefore believe that there is an additional cause of GJIC disruption in WB-F344 cells: the rapid depletion of phosphorylated Cx43 by anisomycin and the subsequent selective regional losses of Cx43 moieties from cell borders. We found that anisomycin treatment could activate Cx43 phosphorylation and this effect was completely inhibited by the pretreatment with SB203580

(Fig. 7C). This result indicated that the anisomycin-induced activation of MAP kinase actually enhanced phosphorylation of Cx43, although it reduced the total amount of Cx43 protein as well as those of P1 and P2. This might indicate the possibility of increased phosphorylation per Cx43 molecule (Lau et al., 1992; Warn-Cramer et al., 1998; Warn-Cramer et al., 1996), although this conclusion needs further study, including the identification of phosphorylated sites. It has been suggested that the degradation of Cx43 depends on increased phosphorylation level of Cx43 (Girão and Pereira, 2003; Guan and Ruch, 1996). Thus, our interpretation of the present result is that MAP-kinase-activated Cx43 phosphorylation might promote the degradation of Cx43.

We found, as have several other groups (Barros et al., 1997; Cano et al., 1994; Cano and Mahadevan, 1995; Hazzalin et al., 1998; Kyriakis et al., 1994), that anisomycin treatment can lead to activation of both p38 MAP kinase and JNK, and that it almost certainly does so by increasing their phosphorylation levels and hence their capacity for enzymatic action. However, we also demonstrated that anisomycin-induced disruption of GJIC was completely blocked in cells pretreated with 10  $\mu\text{M}$  SB203580 (a concentration that had virtually no effect on the anisomycin-induced phosphorylation of JNK). Given these observations, it seems unlikely that the JNK pathway will prove to play a significant role in the anisomycin-induced disruption of GJIC. Thus, even though anisomycin appears to be capable of provoking the phosphorylation – and hence activation – of JNK, it might well be that its ability to inhibit GJIC is due almost entirely to its ability to activate p38 MAP kinase.

In this study, we used a very high concentration (10  $\mu\text{g ml}^{-1}$ ) of anisomycin, primarily because this level was maximally

effective as a GJIC inhibitor in WB-F344 cells (Fig. 2B). We were aware that anisomycin might also act as a translational inhibitor at such concentrations. A previous study (Mahadevan and Edwards, 1991) has shown that relatively low concentrations of anisomycin (around 25–50 ng ml<sup>-1</sup>, so-called subinhibitory levels) can selectively activate the p38 MAP kinase without inhibiting protein synthesis. In our study, however, even a lower concentration of anisomycin (10 ng ml<sup>-1</sup>) appeared to have an ability to inhibit protein synthesis, but this concentration could not activate p38 MAP kinase (Fig. 2B, Fig. 3C). This discrepancy might be due to the different cell lines used in the studies. In any event, GJIC could be maintained at the control level by SB203580 pretreatment without recovery of protein synthesis (Fig. 5D), indicating that the effect of anisomycin on GJIC was not dependent on the inhibition of protein synthesis. Our conclusion gained further support from our observation that SB203580 pretreatment of the cells appeared to be capable of preventing anisomycin-induced losses of the P1 or P2 (but not P0) forms of Cx43. Moreover, both before and after treatment in our experiments, we checked the effects on the intracellular levels of ZO-1, occludin, E-cadherin and  $\beta$ -catenin as reference proteins, which have short half-lives like that of Cx43. We did not detect changes in the levels of these reference proteins in any anisomycin treatment experiment.

Anisomycin is also a well known inducer of apoptosis in other cell lines (Polverino and Patterson, 1997; Stadheim and Kucera, 2002). Furthermore, the up- or downregulation of GJIC has been reported in the apoptotic process (Wilson et al., 2000). However, in our experiment, at least up to 120 minutes, anisomycin did not induce apoptosis in WB-F344 cells (data not shown).

A key finding of our present study is that pretreatment of anisomycin-exposed WB-F344 cells with SB203580 appeared to inhibit both the redistribution of Cx43 derivatives and to ameliorate or prevent the disruption of GJIC that anisomycin would otherwise have provoked. It is also important that the protection against GJIC disruption afforded by SB203580 pretreatment was, for all intents and purposes, complete. Given that SB203580 is reputed to be a highly specific inhibitor of p38 MAP kinase (Cuenda et al., 1995; Tong et al., 1997), it seems likely that the most important single event in the anisomycin-induced disruption of GJIC involves its ability to activate this particular kinase. It remains uncertain whether our interpretation will turn out to be an oversimplification, if only because WB-F344 cells pretreated with SB203580 appear to experience virtually no disruption of GJIC under circumstances in which the inhibition of p38 MAP kinase by SB203580 is not complete. Moreover, western blotting analysis revealed that SB203580 was capable of inhibiting JNK and that inhibition of p38 MAP kinase was incomplete. These observations are in accordance with a report that SB203580 is capable of inhibiting JNK when used at relatively high concentrations (Clerk and Sugden, 1998) and others that SB203580 only appears to exert its inhibitory effect on specific isoforms of p38 MAP kinase (Cuenda et al., 1995; Lee et al., 1994). Suggestions that the p38 MAP kinase and JNK pathways engage in cross talk in response to anisomycin might also be relevant (Töröcsik and Szeberényi, 2000). We are currently conducting additional experiments in the hope of obtaining a more thorough understanding of the mechanisms involved in GJIC inhibition by the p38 MAP kinase pathway.

We thank Baxter Limited Renal Division for their support in conducting this study. This study was supported in part by Grants-in-Aid for Scientific Research from the Ministry of Education, Science, Sports and Culture of Japan, and for Cancer Research from the Ministry of Health and Welfare of Japan, and by a grant from the Smoking Research Foundation. We thank E. Suzuki (Department of Histology and Cell Biology, Hiroshima University School of Medicine, Hiroshima, Japan) and K. Yamashita (Department of Anatomy and Developmental Biology, Hiroshima University School of Medicine, Hiroshima, Japan) for helpful advice.

## References

- Barros, L. F., Young, M., Saklatvala, J. and Baldwin, S. A. (1997). Evidence of two mechanisms for the activation of the glucose transporter GLUT1 by anisomycin: p38(MAP kinase) activation and protein synthesis inhibition in mammalian cells. *J. Physiol.* **504**, 517–525.
- Berthoud, V. M., Rook, M. B., Traub, O., Hertzberg, E. L. and Sáez, J. C. (1993). On the mechanisms of cell uncoupling induced by a tumor promoter phorbol ester in clone 9 cells, a rat liver epithelial cell line. *Eur. J. Cell Biol.* **62**, 384–396.
- Beyer, E. C., Paul, D. L. and Goodenough, D. A. (1987). Connexin43: a protein from rat heart homologous to a gap junction protein from liver. *J. Cell Biol.* **105**, 2621–2629.
- Cano, E., Hazzalin, C. A. and Mahadevan, L. C. (1994). Anisomycin-activated protein kinases p45 and p55 but not mitogen-activated protein kinases ERK-1 and -2 are implicated in the induction of c-Fos and c-Jun. *Mol. Cell Biol.* **14**, 7352–7362.
- Cano, E. and Mahadevan, L. C. (1995). Parallel signal processing among mammalian MAPKs. *Trends Biochem. Sci.* **20**, 117–122.
- Cho, J. H., Cho, S. D., Hu, H., Kim, S. H., Lee, S. K., Lee, Y. S. and Kang, K. S. (2002). The roles of ERK1/2 and p38 MAP kinases in the preventive mechanisms of mushroom *Phellinus linteus* against the inhibition of gap junctional intercellular communication by hydrogen peroxide. *Carcinogenesis* **23**, 1163–1169.
- Clerk, A. and Sugden, P. H. (1998). The p38-MAPK inhibitor, SB203580, inhibits cardiac stress-activated protein kinases/c-Jun N-terminal kinases (SAPKs/JNKs). *FEBS Lett.* **426**, 93–96.
- Cuenda, A., Rouse, J., Doza, Y. N., Meier, R., Cohen, P., Gallagher, T. F., Young, P. R. and Lee, J. C. (1995). SB 203580 is a specific inhibitor of a MAP kinase homologue which is stimulated by cellular stresses and interleukin-1. *FEBS Lett.* **364**, 229–233.
- Dupont, E., el Aoumari, A., Fromaget, C., Briand, J. P. and Gros, D. (1991). Affinity purification of a rat-brain junctional protein, connexin 43. *Eur. J. Biochem.* **200**, 263–270.
- Elvira, M., Díez, J. A., Wang, K. K. and Villalobo, A. (1993). Phosphorylation of connexin-32 by protein kinase C prevents its proteolysis by mu-calpain and m-calpain. *J. Biol. Chem.* **268**, 14294–14300.
- Girão, H. and Pereira, P. (2003). Phosphorylation of connexin 43 acts as a stimulus for proteasome-dependent degradation of the protein in lens epithelial cells. *Mol. Vis.* **9**, 24–30.
- Guan, X. and Ruch, R. J. (1996). Gap junction endocytosis and lysosomal degradation of connexin43-P2 in WB-F344 rat liver epithelial cells treated with DDT and lindane. *Carcinogenesis* **17**, 1791–1798.
- Hazzalin, C. A., le Panse, R., Cano, E. and Mahadevan, L. C. (1998). Anisomycin selectively desensitizes signalling components involved in stress kinase activation and Fos and Jun induction. *Mol. Cell Biol.* **18**, 1844–1854.
- Helliwell, P. A., Richardson, M., Affleck, J. and Kellett, G. L. (2000). Regulation of GLUT5, GLUT2 and intestinal brush-border fructose absorption by the extracellular signal-regulated kinase, p38 mitogen-activated kinase and phosphatidylinositol 3-kinase intracellular signalling pathways: implications for adaptation to diabetes. *Biochem. J.* **350**, 163–169.
- Hii, C. S., Ferrante, A., Edwards, Y. S., Huang, Z. H., Hartfield, P. J., Rathjen, D. A., Poulos, A. and Murray, A. W. (1995a). Activation of mitogen-activated protein kinase by arachidonic acid in rat liver epithelial WB cells by a protein kinase C-dependent mechanism. *J. Biol. Chem.* **270**, 4201–4204.
- Hii, C. S., Ferrante, A., Schmidt, S., Rathjen, D. A., Robinson, B. S., Poulos, A. and Murray, A. W. (1995b). Inhibition of gap junctional communication by polyunsaturated fatty acids in WB cells: evidence that connexin 43 is not hyperphosphorylated. *Carcinogenesis* **16**, 1505–1511.
- Hossain, M. Z., Ao, P. and Boynton, A. L. (1998a). Platelet-derived growth



- factor-induced disruption of gap junctional communication and phosphorylation of connexin43 involves protein kinase C and mitogen-activated protein kinase. *J. Cell Physiol.* **176**, 332-341.
- Hossain, M. Z., Ao, P. and Boynton, A. L. (1998b). Rapid disruption of gap junctional communication and phosphorylation of connexin43 by platelet-derived growth factor in T51B rat liver epithelial cells expressing platelet-derived growth factor receptor. *J. Cell Physiol.* **174**, 66-77.
- Hossain, M. Z., Jagdale, A. B., Ao, P. and Boynton, A. L. (1999a). Mitogen-activated protein kinase and phosphorylation of connexin43 are not sufficient for the disruption of gap junctional communication by platelet-derived growth factor and tetradecanoylphorbol acetate. *J. Cell Physiol.* **179**, 87-96.
- Hossain, M. Z., Jagdale, A. B., Ao, P., Kazlauskas, A. and Boynton, A. L. (1999b). Disruption of gap junctional communication by the platelet-derived growth factor is mediated via multiple signaling pathways. *J. Biol. Chem.* **274**, 10489-10496.
- Kanemitsu, M. Y. and Lau, A. F. (1993). Epidermal growth factor stimulates the disruption of gap junctional communication and connexin43 phosphorylation independent of 12-O-tetradecanoylphorbol 13-acetate-sensitive protein kinase C: the possible involvement of mitogen-activated protein kinase. *Mol. Biol. Cell* **4**, 837-848.
- Kyriakis, J. M., Banerjee, P., Nikolakaki, E., Dai, T., Rubie, E. A., Ahmad, M. F., Avruch, J. and Woodgett, J. R. (1994). The stress-activated protein kinase subfamily of c-Jun kinases. *Nature* **369**, 156-160.
- Laird, D. W., Castillo, M. and Kasprzak, L. (1995). Gap junction turnover, intracellular trafficking, and phosphorylation of connexin43 in brefeldin A-treated rat mammary tumor cells. *J. Cell Biol.* **131**, 1193-1203.
- Lau, A. F., Kanemitsu, M. Y., Kurata, W. E., Danesh, S. and Boynton, A. L. (1992). Epidermal growth factor disrupts gap-junctional communication and induces phosphorylation of connexin43 on serine. *Mol. Biol. Cell* **3**, 865-874.
- Lee, J. C., Laydon, J. T., McDonnell, P. C., Gallagher, T. F., Kumar, S., Green, D., McNulty, D., Blumenthal, M. J., Heys, J. R., Landvatter, S. W. et al. (1994). A protein kinase involved in the regulation of inflammatory cytokine biosynthesis. *Nature* **372**, 739-746.
- Loewenstein, W. R. (1990). Cell-to-cell communication and the control of growth. *Am. Rev. Respir. Dis.* **142**, S48-S53.
- Mahadevan, L. C. and Edwards, D. R. (1991). Signalling and superinduction. *Nature* **349**, 747-748.
- Matesic, D. F., Rupp, H. L., Bonney, W. J., Ruch, R. J. and Trosko, J. E. (1994). Changes in gap-junction permeability, phosphorylation, and number mediated by phorbol ester and non-phorbol-ester tumor promoters in rat liver epithelial cells. *Mol. Carcinog.* **10**, 226-236.
- Minden, A. and Karin, M. (1997). Regulation and function of the JNK subgroup of MAP kinases. *Biochim. Biophys. Acta* **1333**, F85-F104.
- Musil, L. S., Cunningham, B. A., Edelman, G. M. and Goodenough, D. A. (1990). Differential phosphorylation of the gap junction protein connexin43 in junctional communication-competent and -deficient cell lines. *J. Cell Biol.* **111**, 2077-2088.
- Musil, L. S. and Goodenough, D. A. (1991). Biochemical analysis of connexin43 intracellular transport, phosphorylation, and assembly into gap junctional plaques. *J. Cell Biol.* **115**, 1357-1374.
- Musil, L. S. and Goodenough, D. A. (1993). Multisubunit assembly of an integral plasma membrane channel protein, gap junction connexin43, occurs after exit from the ER. *Cell* **74**, 1065-1077.
- Ogawa, T., Hayashi, T., Kyoizumi, S., Ito, T., Trosko, J. E. and Yorioka, N. (1999). Up-regulation of gap junctional intercellular communication by hexamethylene bisacetamide in cultured human peritoneal mesothelial cells. *Lab. Invest.* **79**, 1511-1520.
- Ogawa, T., Hayashi, T., Yorioka, N., Kyoizumi, S. and Trosko, J. E. (2001). Hexamethylene bisacetamide protects peritoneal mesothelial cells from glucose. *Kidney Int.* **60**, 996-1008.
- Polontchouk, L., Ebelt, B., Jackels, M. and Dhein, S. (2002). Chronic effects of endothelin 1 and angiotensin II on gap junctions and intercellular communication in cardiac cells. *FASEB J.* **16**, 87-89.
- Polverino, A. J. and Patterson, S. D. (1997). Selective activation of caspases during apoptotic induction in HL-60 cells. Effects of a tetrapeptide inhibitor. *J. Biol. Chem.* **272**, 7013-7021.
- Ruch, R. J., Trosko, J. E. and Madhukar, B. V. (2001). Inhibition of connexin43 gap junctional intercellular communication by TPA requires ERK activation. *J. Cell Biochem.* **83**, 163-169.
- Seger, R. and Krebs, E. G. (1995). The MAPK signaling cascade. *FASEB J.* **9**, 726-735.
- Stadheim, T. A. and Kucera, G. L. (2002). c-Jun N-terminal kinase/stress-activated protein kinase (JNK/SAPK) is required for mitoxantrone- and anisomycin-induced apoptosis in HL-60 cells. *Leukocyte Res.* **26**, 55-65.
- Tong, L., Pav, S., White, D. M., Rogers, S., Crane, K. M., Cywin, C. L., Brown, M. L. and Pargellis, C. A. (1997). A highly specific inhibitor of human p38 MAP kinase binds in the ATP pocket. *Nat. Struct. Biol.* **4**, 311-316.
- Töröcsik, B. and Szeberényi, J. (2000). Anisomycin uses multiple mechanisms to stimulate mitogen-activated protein kinases and gene expression and to inhibit neuronal differentiation in PC12 pheochromocytoma cells. *Eur. J. Neurosci.* **12**, 527-532.
- Trosko, J. E., Chang, C. C., Wilson, M. R., Upham, B., Hayashi, T. and Wade, M. (2000). Gap junctions and the regulation of cellular functions of stem cells during development and differentiation. *Methods* **20**, 245-264.
- Trosko, J. E. and Ruch, R. J. (1998). Cell-cell communication in carcinogenesis. *Front. Biosci.* **3**, 208-236.
- Tsao, M. S., Smith, J. D., Nelson, K. G. and Grisham, J. W. (1984). A diploid epithelial cell line from normal adult rat liver with phenotypic properties of 'oval' cells. *Exp. Cell Res.* **154**, 38-52.
- Wade, M. H., Trosko, J. E. and Schindler, M. (1986). A fluorescence photobleaching assay of gap junction-mediated communication between human cells. *Science* **232**, 525-528.
- Warn-Cramer, B. J., Cottrell, G. T., Burt, J. M. and Lau, A. F. (1998). Regulation of connexin-43 gap junctional intercellular communication by mitogen-activated protein kinase. *J. Biol. Chem.* **273**, 9188-9196.
- Warn-Cramer, B. J., Lampe, P. D., Kurata, W. E., Kanemitsu, M. Y., Loo, L. W., Eckhart, W. and Lau, A. F. (1996). Characterization of the mitogen-activated protein kinase phosphorylation sites on the connexin-43 gap junction protein. *J. Biol. Chem.* **271**, 3779-3786.
- Wilson, M. R., Close, T. W. and Trosko, J. E. (2000). Cell population dynamics (apoptosis, mitosis, and cell-cell communication) during disruption of homeostasis. *Exp. Cell Res.* **254**, 257-268.

## Caspase-2 and Caspase-7 Are Involved in Cytolethal Distending Toxin-Induced Apoptosis in Jurkat and MOLT-4 T-Cell Lines

Masaru Ohara,<sup>1</sup> Tomonori Hayashi,<sup>2</sup> Yoichiro Kusunoki,<sup>2</sup> Mutsumi Miyauchi,<sup>3</sup>  
Takashi Takata,<sup>3</sup> and Motoyuki Sugai<sup>1\*</sup>

Departments of Bacteriology<sup>1</sup> and Oral Maxillofacial Pathology,<sup>3</sup> Hiroshima University Graduate School of Biomedical Sciences, Hiroshima 734-8553, and Department of Radiobiology and Molecular Epidemiology, Radiation Effects Research Foundation, Hiroshima 732-0815,<sup>2</sup> Japan

Received 20 May 2003/Returned for modification 12 August 2003/Accepted 22 October 2003

Cytolethal distending toxin (CDT) from *Actinobacillus actinomycetemcomitans* is a G<sub>2</sub>/M cell-cycle-specific growth-inhibitory toxin that leads to target cell distension followed by cell death. To determine the mechanisms by which *A. actinomycetemcomitans* CDT acts as an immunosuppressive factor, we examined the effects of highly purified CDT holotoxin on human T lymphocytes. Purified CDT was cytolethal toward normal peripheral T lymphocytes that were activated by in vitro stimulation with phytohemagglutinin. In addition, purified CDT showed cytolethal activity against Jurkat and MOLT-4 cells, which are known to be sensitive and resistant, respectively, to Fas-mediated apoptosis. Death in these cell lines was accompanied by the biochemical features of apoptosis, including membrane conformational changes, intranucleosomal DNA cleavage, and an increase in caspase activity in the cells. Pretreatment of Jurkat cells with the general caspase inhibitor z-VAD-fmk mostly suppressed CDT-induced apoptosis. Furthermore, specific inhibitors of caspase-2 and -7 showed significant inhibitory effects on CDT-induced apoptosis in Jurkat cells, and these inhibitory effects were fully associated with reduced activity of caspase-2 or -7 in the CDT-treated Jurkat cells. These results strongly suggest that CDT possesses the ability to induce human T-cell apoptosis through activation of caspase-2 and -7.

Bacterial infections in mammals evoke a series of immune reactions to bacterial antigens in the infected host, but immune responses are occasionally suppressed or shut down by some bacterial products, such as toxins. Suppression or inactivation of the host immune response is considered to be a bacterial strategy to evade host immune mechanisms. *Actinobacillus actinomycetemcomitans* is a gram-negative rod-shaped pathogen implicated in the pathogenesis of juvenile and adult periodontitis (38). Previous studies demonstrated that *A. actinomycetemcomitans* produces a factor(s) that is immunosuppressive for human T and B cells (25). It was recently established that *A. actinomycetemcomitans* produces a new member of the cytolethal distending toxin (CDT) family which was previously unrecognized as a virulence factor of *A. actinomycetemcomitans* (40). CDT belongs to the family of toxins with cell-cycle-specific inhibitory activities which block the progression of cells from G<sub>2</sub> to M phase (28). CDT-poisoned cells undergo cell distension and nucleus swelling and eventually die. CDT was found to form a complex of three subunits, CDTA, -B, and -C (9, 14, 21, 24, 31, 40), and the subunits were determined to be tandemly encoded by the *cdtA*, *cdtB*, and *cdtC* genes at the chromosomal *cdt* loci. *A. actinomycetemcomitans* CDTA, -B, and -C are translated as approximately 25-, 32-, and 21-kDa proteins, respectively, and are secreted into the periplasm (40). After cleavage of their 15- to 21-amino-acid signal sequences at the N terminus, they become 23-, 29-, and 19-kDa proteins, respectively (31, 36, 40). CDTA goes through another process-

ing step to become an 18- to 19-kDa form, designated CDTA', and forms a complex with CDTB and CDTC to become a holotoxin (40).

In 1999, Shenker et al. purified the immunosuppressive factor of *A. actinomycetemcomitans* that could affect human T cells and demonstrated that the factor was one of the subunit proteins of CDT, CDTB (34, 36). Their group also demonstrated that a crude CDT preparation of *A. actinomycetemcomitans* induced cell cycle arrest at the G<sub>2</sub> phase in human peripheral blood cells (37). Furthermore, the CDT preparation was shown to induce apoptotic cell death in peripheral blood lymphocytes along with activation of caspase-3, -8, and -9 (35). Despite those findings, whether these caspases are really involved in CDT-induced apoptosis remains virtually unknown.

For this study, we studied the immunosuppressive effect of highly purified *A. actinomycetemcomitans* CDT on normal human T lymphocytes and made an in-depth characterization of the cytolethal effect by using the T-cell leukemia cell lines Jurkat and MOLT-4, which are sensitive and resistant, respectively, to Fas-mediated apoptosis. We herein demonstrate that CDT induces apoptosis in these cells and that caspase-2 and -7 play important roles in the signaling pathway of CDT-induced cell death, which is distinct from Fas-mediated apoptosis.

### MATERIALS AND METHODS

**Purification of *A. actinomycetemcomitans* CDT.** CDT holotoxin was prepared by using the pQE 60 (C-terminal histidine tag) protein expression system in M15 *Escherichia coli* (Qiagen, Tokyo, Japan). Briefly, for construction of pQEcdtABC, the *A. actinomycetemcomitans* *cdtABC* gene was isolated from *A. actinomycetemcomitans* genomic DNA by PCR amplification with specific primers that contained several restriction enzyme sites for subcloning into vectors, as follows: QIA-U, 5'-AGGTACCATGGAAAAGTTT-3', which corresponds to the *cdtA* starting site with an *Nco*I restriction enzyme site; QIC-L, 5'-AAAGATCTGCT ACCCTGA-3', which corresponds to the end of the *cdtC* gene, with the stop

\* Corresponding author. Mailing address: Department of Bacteriology, Hiroshima University Graduate School of Biomedical Sciences, Sumi 1-2-3, Minami-ku, Hiroshima, Hiroshima 734-8553, Japan. Phone: (81) 82 257 5635. Fax: (81) 82 257 5639. E-mail: sugai@hiroshima-u.ac.jp.

codon replaced with a *Bgl*II site (restriction sites are shown in italics). The amplified *cdtABC* gene was ligated into pQE60 in frame at the *Nco*I and *Bgl*II sites, so that the C-terminal CDTC was tagged with six histidine residues. The expression of the *cdtABC* gene was induced by adding isopropyl- $\beta$ -D-1-thiogalactopyranoside (final concentration of 1 mM; Sigma) at an optical density at 660 nm of 0.5 to 0.7. After induction for 4 h, the culture supernatant was harvested by centrifugation at  $5,000 \times g$  for 5 min, and crude proteins were precipitated with ammonium sulfate (final concentration, 80%) by gentle stirring for at least 4 h. The precipitates were recovered by centrifugation at  $15,000 \times g$  for 20 min, dissolved in phosphate-buffered saline (PBS) (137 mM NaCl, 2.7 mM KCl, 8.1 mM  $\text{Na}_2\text{HPO}_4$ , 1.5 mM  $\text{KH}_2\text{PO}_4$ ), and dialyzed overnight against PBS. Nickelated agarose beads were added into the dialyzed solution and gently shaken for at least 1 h, followed by column chromatography. The column was washed with washing buffer (50 mM  $\text{NaH}_2\text{PO}_4$  [pH 8.0], 300 mM NaCl, 20 mM imidazole) and eluted with elution buffer (50 mM  $\text{NaH}_2\text{PO}_4$  [pH 8.0], 300 mM NaCl, 250 mM imidazole). The eluted CDT holotoxin was dialyzed against PBS and concentrated with Centricon 10 concentrators (Millipore, Bedford, Mass.).

**Preparation of cells and culture conditions.** Peripheral blood mononuclear cells were obtained from healthy volunteers with their informed consent. Twenty to forty milliliters of heparinized venous blood was diluted with an equal volume of PBS with 1% heparin and layered over Ficoll-Hypaque lymphocyte separation medium (ICN Biomedical Inc., Aurora, Ohio). Density gradient centrifugation was performed at  $400 \times g$  for 30 min, and mononuclear cells were harvested from the plasma-lymphocyte separation medium interface. Collected cells were washed twice with Earle's balanced salt solution (Nissui, Tokyo, Japan) containing 2.5% fetal calf serum (FCS) (Intergen Co., Purchase, N.Y.). The number of recovered cells was counted and diluted to  $10^6$  cells/ml in RPMI 1640 containing 10% FCS, 100 U of penicillin G/ml, and 100  $\mu\text{g}$  of streptomycin/ml. The isolated lymphocytes were incubated with CDT (100 ng/ml) and cultured at 37°C in 5%  $\text{CO}_2$ , with or without stimulation on day 1 by phytohemagglutinin (PHA) (Difco Lab., Detroit, MI) diluted 1:1,600, and the cell population was monitored for 96 h. A thymic T-cell leukemia cell line, MOLT-4, and a peripheral T-cell leukemia cell line, Jurkat, were maintained in RPMI 1640 containing 10% FCS and 25  $\mu\text{g}$  of kanamycin/ml at 37°C in 5%  $\text{CO}_2$ . The cells ( $10^6$  cells/ml) were left untreated or were treated with CDT (100 ng/ml) and cultured under similar conditions. In some experiments, Jurkat cells were similarly treated with 100 ng of anti-CD95 (anti-Fas) monoclonal antibody (Ab) CH11 (BD Pharmingen, San Diego, Calif.) per ml.

**Flow cytometry.** Conformational changes of the membrane by phosphatidylserine translocation and membrane hole formation were observed by counting the percentages of cells that were stained with fluorescein isothiocyanate (FITC)-labeled annexin V and propidium iodide (PI) in a FACScan flow cytometer (BD Biosciences, San Jose, Calif.). Briefly, CDT-treated cells ( $5 \times 10^5$  to  $10 \times 10^5$ ) were collected by centrifugation at  $350 \times g$  for 2 min and were washed three times with 500  $\mu\text{l}$  of PBS with 1% FCS. The washed cells were resuspended in 180  $\mu\text{l}$  of PBS with 1% FCS, and 0.5  $\mu\text{l}$  of FITC-labeled annexin V and 1  $\mu\text{l}$  of PI, from the MEBCYTO apoptosis kit (MBL, Nagoya, Japan) were added to the cell suspension. After the reaction for 5 min at room temperature, 10,000 cells were analyzed in the FACScan instrument. The data obtained were processed by quadrant population analysis, using CellQuest software (BD Biosciences). The living cell population was determined by counting cells that were negative for both annexin V and PI (distributed in the lower left of the quadrant).

**Caspase assay.** CDT-treated cells were harvested and washed with PBS. PBS-washed cells were lysed with lysis buffer (10 mM Tris-Cl [pH 7.4], 25 mM NaCl, 0.25% Triton X-100, 1 mM EDTA) and centrifuged at  $15,000 \times g$  for 10 min. The supernatant was diluted with the lysis buffer and the protein concentration was adjusted to 1 mg/ml. Ten micrograms of total protein was incubated in 200  $\mu\text{l}$  of caspase buffer (50 mM Tris-Cl [pH 7.2], 100 mM NaCl, 1 mM EDTA, 10% sucrose, 0.1% CHAPS, and 5 mM dithiothreitol) with a 50  $\mu\text{M}$  concentration (each) of various fluorogenic substrate peptides. The peptides include Ac-DEVD-7-amino-4-methylcumarine (AMC) for caspase-3, -7, and -8, Ac-DQTD-AMC for caspase-7 and -3, Ac-IETD-AMC for caspase-8, -6, and granzyme, Ac-LEHD-AMC for caspase-9, and Ac-VDVAD-AMC for caspase-2 (Peptide Institute Inc., Osaka, Japan).

The reaction mixture was incubated at 37°C for 60 min, and the release of 7-amino-4-methylcumarin was measured by use of a spectrophotometer (Shimadzu RF-540), with excitation at 380 nm and emission at 460 nm. One unit (U) was defined as 5.2 pmol of substrate cleaved per min per mg of protein.

Various caspase inhibitors were used at a concentration of 100  $\mu\text{M}$ . They were Ac-VAD-fmk as a general caspase inhibitor, Ac-WEHD-CHO for caspase-1, Ac-DEVD-CHO for caspase-3, -7, and -8, Ac-DMQD-CHO for caspase-3, Ac-LEHD-CHO for caspase-9, Ac-IETD-CHO for caspase-8 and -6, Ac-DQTD-

CHO for caspase-7 and -3, and Ac-VDVAD-CHO for caspase-2 (Peptide Institute Inc.).

**Electron microscopy.** Cells were fixed with 2.5% glutaraldehyde for 2 h and rinsed in 0.1 M cacodylate buffer (pH 7.4) for 12 h. After postfixation with 1% osmium tetroxide for 30 min, cells were stained with 2% uranyl acetate for 30 min and dehydrated in graded alcohol, which was then replaced by propylene oxide. After these steps, the cell suspension was spun down at  $8,000 \times g$  for 5 min and the supernatant was discarded. The cell pellets were embedded in epoxy resin. Thin sections were stained in 2% uranyl acetate and lead citrate and were observed in a Hitachi H500 electron microscope.

**Preparation of cytosolic and mitochondrial fractions.** CDT-treated cells were washed twice with PBS and resuspended in isotonic buffer (10 mM HEPES [pH 7.3], 0.3 M mannitol, 0.1% bovine serum albumin). Digitonin was added to the cell suspension at a concentration of 0.1 mM, and the cells were incubated for 5 min on ice. After the samples were centrifuged at  $8,500 \times g$  for 5 min at 4°C, the supernatant was used as the cytosolic fraction. The pellet was resuspended in sonication buffer (50 mM Tris-HCl [pH 7.4], 150 mM NaCl, 2 mM EDTA, 1 mM phenylmethylsulfonyl fluoride, 0.5% Tween 20). The samples were sonicated with an ultrasonic disrupter (UD200 TOMY) for 20 s at output level 4. After centrifugation at  $10,000 \times g$  for 5 min at 4°C, the supernatant was collected and used as the mitochondrial fractions.

**Antibodies.** Antibodies against CDTA, -B, and -C that were previously obtained were used under conditions that were described elsewhere (40). Anti-cytochrome c Ab (BD Pharmingen) was used according to the instructions provided by the supplier.

## RESULTS

**Cytolethal effects of highly purified CDT on human peripheral lymphocytes.** *A. actinomycetemcomitans* CDT was purified from the culture supernatant of *E. coli* carrying the *A. actinomycetemcomitans cdtABC* genes. The secreted CDT complex was purified through a Ni chelation column, using the affinity of six histidine (His) residues tagged to the C terminus of CDTC (Fig. 1A). Sodium dodecyl sulfate-polyacrylamide gel electrophoresis and immunoblotting detected CDTA', CDTB, and CDTC tagged with six histidine residues in the medium fraction, and premature CDTA was also found in a small amount, suggesting that most of the CDT complex consisted of CDTA', CDTB, and CDTC. Cell distension and the  $G_2/M$  blocking activity of purified CDT were confirmed in HeLa cells, and the purified CDT complex was used for experiments.

To address whether CDT can induce cell death of human peripheral lymphocytes, we added purified CDT to peripheral blood mononuclear cell cultures in the presence or absence of PHA stimulation. Flow cytometry analysis with FITC-annexin V and PI revealed that treatment of normal lymphocytes with a combination of CDT and PHA increased the percentage of dead cells (the sum of annexin V<sup>+</sup> PI<sup>+</sup> and annexin V<sup>+</sup> PI<sup>-</sup> fractions) (Fig. 1B). It should be noted that CDT did not kill lymphocytes very much unless they were activated with PHA. This is in good agreement with the previously suggested activity of CDT, which is cell-cycle-dependent cytotoxicity against HeLa cells (1), and also suggests that CDT can act as an immunosuppressive toxin by killing activated lymphocytes.

**CDT induced apoptosis in Jurkat and MOLT-4 cells.** In order to obtain further insights into the cytolethal effect of CDT in T lymphocytes, we used two cell lines, Jurkat and MOLT-4, and monitored population changes in four panels (upper left, upper right, lower left, and lower right [UL, UR, LL, and LR, respectively]) after CDT treatment (Fig. 2). For both cell lines, CDT treatment increased the percentage of dead cells (Fig. 2A). Flow cytometry analysis revealed that the percentage of annexin V<sup>+</sup> PI<sup>-</sup> Jurkat cells (distributed in the

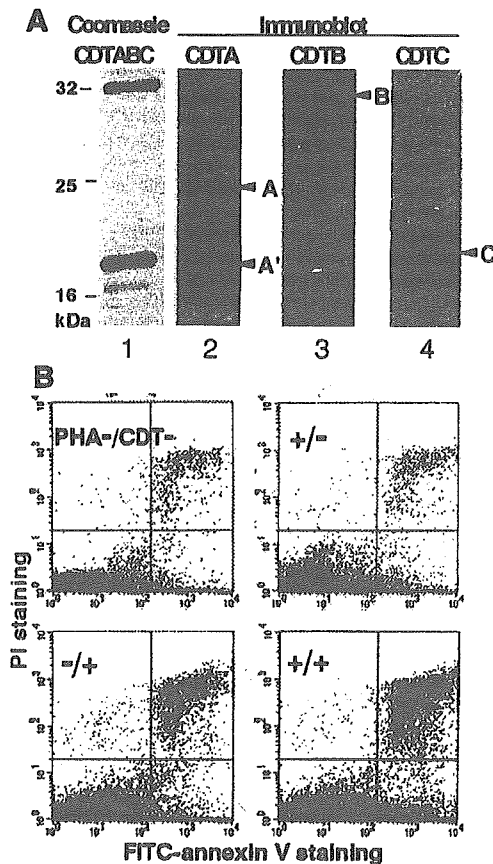


FIG. 1. Cytolethal effect of *A. actinomycetemcomitans* CDT on human peripheral lymphocytes. (A) Purified CDTABC complex in the medium fraction from *E. coli* M15 carrying *A. actinomycetemcomitans* *cdtABC*. Lane 1, Coomassie staining of CDTABC complex; lanes 2 to 4, immunoblots for the detection of each subunit by use of antiserum against CDTA, CDTB, and CDTC, respectively. Arrowheads: A, CDTA (premature form); A', CDTA' (mature form of CDTA); B, mature CDTB; C, mature CDTC tagged with six histidine residues. (B) Flow cytometry analysis. Lymphocytes were stained with FITC-labeled annexin V and PI and analyzed in a FACScan flow cytometer. Lymphocytes prepared from peripheral blood obtained from healthy human volunteers were treated with several combinations of PHA (1:1,600) and CDT (100 ng/ml). A representative result of the quadrant analysis of annexin V- and PI-stained lymphocytes on day 2 is shown.

LR panel) started to increase 8 h after CDT treatment and continued to increase until 24 h after treatment (Fig. 2B). MOLT-4 showed a somewhat different pattern from that of Jurkat. The percentage of annexin V<sup>+</sup> PI<sup>-</sup> MOLT-4 cells (LR) started to increase 4 h after CDT treatment and reached a plateau 12 to 16 h after the treatment (Fig. 2B). After that, the annexin V<sup>+</sup> PI<sup>-</sup> population (LR) decreased after 16 h. Concomitantly with the increase and decrease of the annexin V<sup>+</sup> PI<sup>-</sup> population (LR), the annexin V<sup>+</sup> PI<sup>+</sup> population (UR) started to increase after 8 h and kept increasing until 24 h. In both cell lines, the increase of the annexin V<sup>+</sup> PI<sup>-</sup> cell population (LR) in the early stage after treatment strongly suggested that CDT poisoning was able to induce apoptosis in cells that are sensitive to Fas-mediated apoptosis as well as in

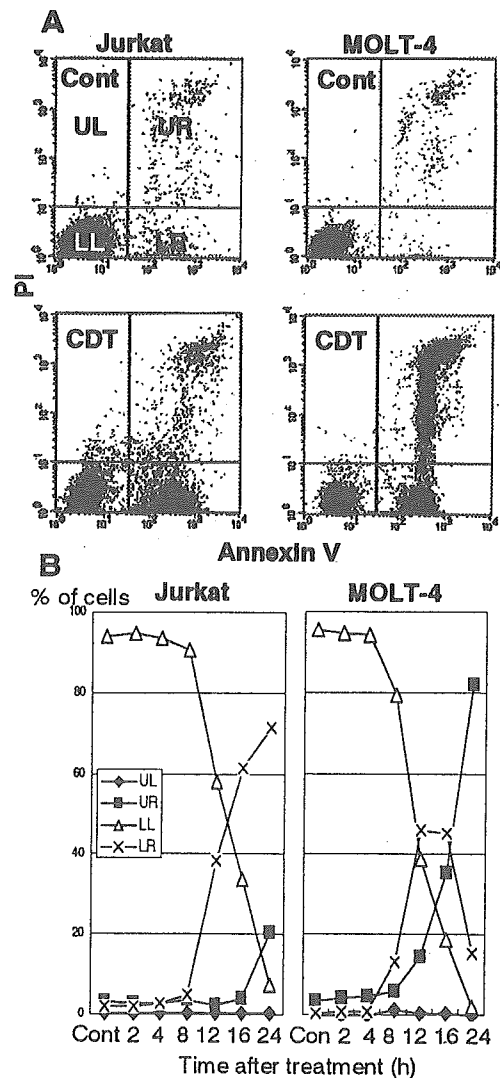


FIG. 2. Cytolethal kinetics on CDT-treated cell lines. T-cell leukemia cell lines Jurkat and MOLT-4 were treated with CDT (100 ng/ml) for various times. Cells stained with FITC-labeled annexin V and PI were analyzed by flow cytometry. (A) Representative results for cells with or without treatment of CDT at 16 h. Cont, control. (B) Kinetics of cell death measured at indicated times after CDT treatment. The percentages of cell populations in the UL quadrant (annexin V<sup>-</sup> PI<sup>+</sup>,  $\diamond$ ), the UR quadrant (annexin V<sup>+</sup> PI<sup>+</sup>,  $\blacksquare$ ), the LL quadrant (annexin V<sup>-</sup> PI<sup>-</sup>,  $\triangle$ ), and the LR quadrant (annexin V<sup>+</sup> PI<sup>-</sup>,  $\times$ ) are indicated.

those that are resistant to Fas-mediated apoptosis. We further investigated the apoptotic characteristics of CDT-poisoned cells, including chromosomal DNA fragmentation and chromatin condensation. As shown in Fig. 3A, electrophoretic analysis of the chromosomal DNA of Jurkat cells showed a typical DNA ladder formation after 16 h of treatment with CDT, which is similar to those observed after treatment with anti-Fas Ab or irradiation. Electron microscopic observation of CDT-poisoned Jurkat cells revealed chromatin condensation, which is associated with cells undergoing apoptosis (Fig. 3B). Similar apoptotic characteristics were also apparent for CDT-treated MOLT-4 cells (data not shown). There was no necrotic change,